

University of Anbar  
Engineering college  
Department of dams and water resources



# REMOTE SENSING AND GIS LECTURES

BY Dr. KHAMIS NABA SAYL

Fourth stage

## List of continent

Chapter one	<b>Concepts and Foundations of Remote Sensing</b> 1.1 Introduction 1.2 Energy Sources and Radiation Principles 1.3 Energy Interactions in the Atmosphere 1.4 Energy Interactions with Earth Surface Features 1.5 Data Acquisition and Digital Image Concepts 1.6 Reference Data 1.7 Characteristics of Remote Sensing Systems 1.8 Successful Application of Remote Sensing 1.9 Geographic Information Systems (GIS) 1.10 Spatial Data Frameworks for GIS and Remote Sensing 1.11 Visual Image Interpretation
Chapter two	<b>Elements of Photographic Systems</b> 2.1 Introduction 2.2 Film Photography 2.3 Digital Photography 2.4 Aerial Cameras 2.5 Spatial Resolution of Camera Systems 2.7 Aerial Videography 2.9 Conclusion
Chapter three	<b>Basic Principles of Photogrammetry</b> 1 Introduction 3.2 Basic Geometric Characteristics of Aerial Photographs 3.3 Photographic Scale 3.4 Ground Coverage of Aerial Photographs 3.5 Area Measurement 3.6 Relief Displacement of Vertical Features 3.7 Image Parallax 3.8 Ground Control for Aerial Photography 3.9 Determining the Elements of Exterior Orientation of Aerial Photographs 3.10 Production of Mapping Products from Aerial Photographs 3.11 Flight Planning 3.12 Conclusion
Chapter four	<b>Earth Resource Satellites Operating in the Optical Spectrum</b> 4.1 Introduction 4.2 General Characteristics of Satellite Remote Sensing Systems Operating in the Optical Spectrum 4.3 Moderate Resolution Systems 4.4 Landsat-1 to -7 4.5 Landsat-8 4.6 Future Landsat Missions and the Global Earth Observation System of Systems 4.7 SPOT-1 to -5 4.8 SPOT-6 and -7 4.9 Evolution of Other Moderate Resolution Systems 339
Chapter five	<b>Microwave and Lidar Sensing</b>
Chapter six	<b>Digital Image Analysis</b>
Chapter seven	<b>APPLICATIONS OF REMOTE SENSING</b>

# المحاضرة

## الأولى

**CONCEPTS AND FOUNDATIONS OF REMOTE SENSING**

## Chapter one

### CONCEPTS AND FOUNDATIONS OF REMOTE SENSING

#### 1.1 INTRODUCTION

Remote sensing is the science and art of obtaining information about an object, area, or phenomenon through the analysis of data acquired by a device that is not in contact with the object, area, or phenomenon under investigation. As you read these words, you are employing remote sensing. Your eyes are acting as sensors that respond to the light reflected from this page. The “data” your eyes acquire are impulses corresponding to the amount of light reflected from the dark and light areas on the page. These data are analyzed, or interpreted, in your mental computer to enable you to explain the dark areas on the page as a collection of letters forming words. Beyond this, you recognize that the words form sentences, and you interpret the information that the sentences convey. In many respects, remote sensing can be thought of as a reading process. Using various sensors, we remotely collect data that may be analyzed to obtain information about the objects, areas, or phenomena being investigated. The remotely collected data can be of many forms, including variations in force distributions, acoustic wave distributions, or electromagnetic energy distributions.

#### Overview of the Electromagnetic Remote Sensing Process

This lecture is about electromagnetic energy sensors that are operated from airborne and spaceborne platforms to assist in inventorying, mapping, and monitoring earth resources. These sensors acquire data on the way various earth surface features emit and reflect electromagnetic energy, and these data are analyzed to provide information about the resources under investigation. Figure 1.1 schematically illustrates the generalized processes and elements involved in electromagnetic remote sensing of earth resources. The two basic processes involved are data acquisition and data analysis. The elements of the data acquisition process are energy sources (a), propagation of energy through the atmosphere (b), energy interactions with earth surface features (c), retransmission of energy through the atmosphere (d), airborne and/or spaceborne sensors (e), resulting in the generation of sensor data in pictorial and/or digital form (f). In short, we use sensors to record variations in the way earth surface features reflect and emit electromagnetic energy. The data analysis process (g) involves examining the data using various viewing and interpretation devices to analyze pictorial data and/or a computer to analyze digital sensor data. Reference data about the resources being studied (such as soil maps, crop statistics, or field-check data) are used when and where available to assist in the data analysis. With the aid of the reference data, the analyst extracts information about the type, extent, location, and condition of the various resources over which the sensor data were collected. This information is then compiled (h), generally in the form of maps, tables, or digital spatial data that can be merged with other “layers” of information in a geographic information system (GIS). Finally, the information is presented to users (i), who apply it to their decision-making process.

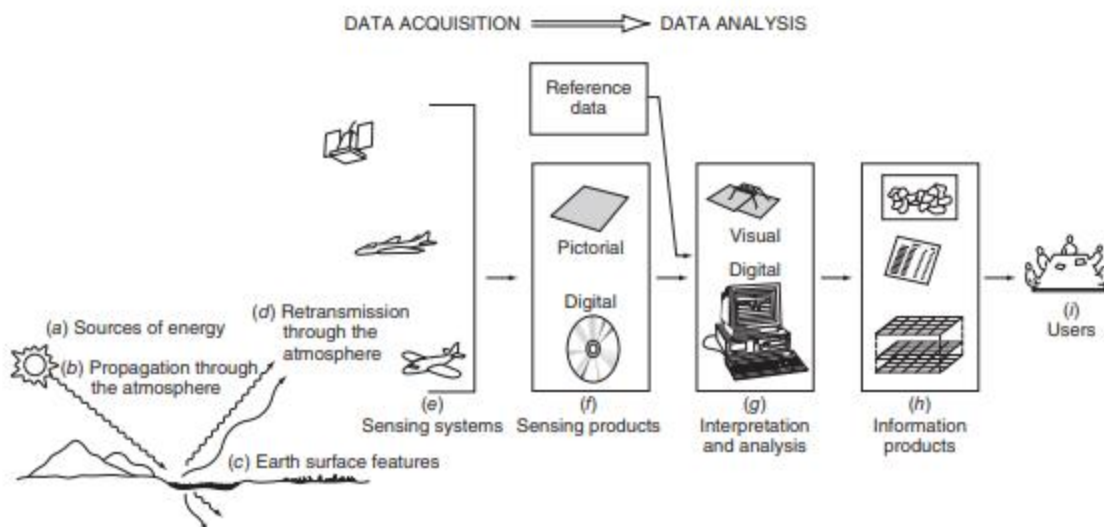


Figure 1.1 Electromagnetic remote sensing of earth resources.

## 1.2 ENERGY SOURCES AND RADIATION PRINCIPLES

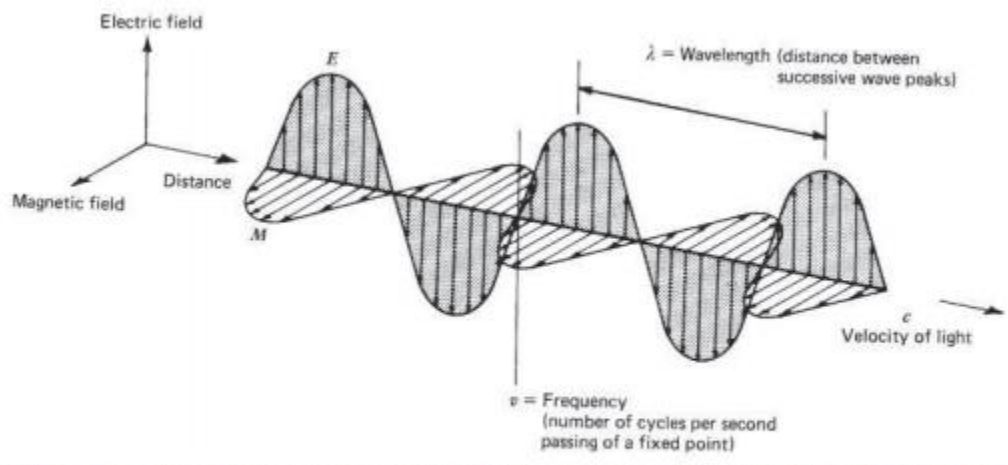
Visible light is only one of many forms of electromagnetic energy. Radio waves, ultraviolet rays, radiant heat, and X-rays are other familiar forms. All this energy is inherently similar and propagates in accordance with basic wave theory. As shown in Figure 1.2, this theory describes electromagnetic energy as traveling in a harmonic, sinusoidal fashion at the “velocity of light”  $c$ . The distance from one wave peak to the next is the wavelength  $\lambda$ , and the number of peaks passing a fixed point in space per unit time is the wave frequency  $\nu$ . From basic physics, waves obey the general equation

$$c = \nu\lambda \quad (1)$$

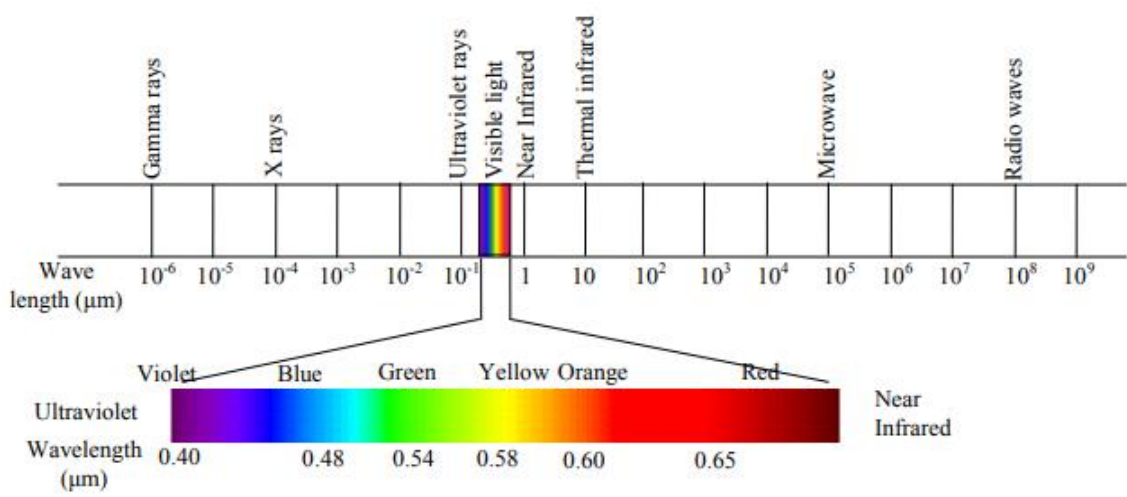
Because  $c$  is essentially a constant  $3 \times 10^8 \text{ m/sec}$ , frequency  $\nu$  and wavelength  $\lambda$  for any given wave are related inversely, and either term can be used to characterize a wave. In remote sensing, it is most common to categorize electromagnetic waves by their wavelength location within the electromagnetic spectrum (Figure 1.3). The most prevalent unit used to measure wavelength along the spectrum is the micrometer  $\mu\text{m}$ . A micrometer equals  $1 \times 10^6 \text{ m}$ .

Although names (such as “ultraviolet” and “microwave”) are generally assigned to regions of the electromagnetic spectrum for convenience, there is no clear-cut dividing line between one nominal spectral region and the next. Divisions of the spectrum have grown from the various methods for sensing each type of radiation more so than from inherent differences in the energy characteristics of various wavelengths. Also, it should be noted that the portions of the electromagnetic spectrum used in remote sensing lie along a continuum characterized by magnitude changes of many powers of 10. Hence, the use of logarithmic plots to depict the electromagnetic spectrum is quite common. The “visible” portion of such a plot is an extremely small one, because the spectral sensitivity of the human eye extends only from about  $0.4 \mu\text{m}$  to approximately  $0.7 \mu\text{m}$ . The color “blue” is ascribed to the approximate range of  $0.4$  to  $0.5 \mu\text{m}$ , “green” to  $0.5$  to  $0.6 \mu\text{m}$ , and “red” to  $0.6$  to  $0.7 \mu\text{m}$ . Ultraviolet (UV) energy adjoins the blue end of the visible portion of the spectrum. Beyond the red end of the visible region are three different categories of infrared (IR) waves: near IR (from  $0.7$  to  $1.3 \mu\text{m}$ ), mid IR (from  $1.3$  to  $3 \mu\text{m}$ ; also referred to as

shortwave IR or SWIR), and thermal IR (beyond 3 to 14  $\mu\text{m}$ , sometimes referred to as longwave IR). At much longer wavelengths (1 mm to 1 m) is the microwave portion of the spectrum.



**Figure 1.2** Electromagnetic wave. Components include a sinusoidal electric wave (E) and a similar magnetic wave (M) at right angles, both being perpendicular to the direction of propagation.



**Figure 1.3** Electromagnetic spectrum.

Most common sensing systems operate in one or several of the visible, IR, or microwave portions of the spectrum. Within the IR portion of the spectrum, it should be noted that only thermal-IR energy is directly related to the sensation of heat; near- and mid-IR energy are not.

Although many characteristics of electromagnetic radiation are most easily described by wave theory, another theory offers useful insights into how electromagnetic energy interacts with matter. This theory—the particle theory—suggests that electromagnetic radiation is composed of many discrete units called photons or quanta. The energy of a quantum is given as

$$Q = hv \quad (1.2)$$

where

- $Q$  = energy of a quantum, joules (J)
- $h$  = Planck's constant,  $6.626 \times 10^{-34}$  J sec
- $\nu$  = frequency

We can relate the wave and quantum models of electromagnetic radiation behavior by solving Eq. 1.1 for  $\nu$  and substituting into Eq. 1.2 to obtain

$$Q = \frac{hc}{\lambda} \quad (1.3)$$

Thus, we see that the energy of a quantum is inversely proportional to its wavelength. The longer the wavelength involved, the lower its energy content. This has important implications in remote sensing from the standpoint that naturally emitted long wavelength radiation, such as microwave emission from terrain features, is more difficult to sense than radiation of shorter wavelengths, such as emitted thermal IR energy. The low energy content of long wavelength radiation means that, in general, systems operating at long wavelengths must “view” large areas of the earth at any given time in order to obtain a detectable energy signal. The sun is the most obvious source of electromagnetic radiation for remote sensing. However, all matter at temperatures above absolute zero (0 K, or -273C) continuously emits electromagnetic radiation. Thus, terrestrial objects are also sources of radiation, although it is of considerably different magnitude and spectral composition than that of the sun. How much energy any object radiates is, among other things, a function of the surface temperature of the object. This property is expressed by the Stefan–Boltzmann law, which states that

$$M = \sigma T^4 \quad (1.4)$$

where

- $M$  = total radiant exitance from the surface of a material, watts (W)  $m^{-2}$
- $\sigma$  = Stefan–Boltzmann constant,  $5.6697 \times 10^{-8}$  W  $m^{-2}$  K $^{-4}$
- $T$  = absolute temperature (K) of the emitting material

The particular units and the value of the constant are not critical for the student to remember, yet it is important to note that the total energy emitted from an object varies as  $T^4$  and therefore increases very rapidly with increases in temperature. Also, it should be noted that this law is expressed for an energy source that behaves as a blackbody. A blackbody is a hypothetical, ideal radiator that totally absorbs and reemits all energy incident upon it. Actual objects only approach this ideal. Suffice it to say for now that the energy emitted from an object is primarily a function of its temperature, as given by Eq. 1.4.

Just as the total energy emitted by an object varies with temperature, the spectral distribution of the emitted energy also varies. Figure 1.4 shows energy distribution curves for blackbodies at temperatures ranging from 200 to 6000 K. The units on the ordinate scale W  $m^{-2}m^{-1}$  express the radiant power coming

from a blackbody per 1- $\mu\text{m}$  spectral interval. Hence, the area under these curves equals the total radiant exitance,  $M$ , and the curves illustrate graphically what the Stefan–Boltzmann law expresses mathematically: The higher the temperature of the radiator, the greater the total amount of radiation it emits. The curves also show that there is a shift toward shorter wavelengths in the peak of a blackbody radiation distribution as temperature increases. The dominant wavelength, or wavelength at which a blackbody radiation curve reaches a maximum, is related to its temperature by Wien’s displacement law,

$$\lambda_m = \frac{A}{T} \quad (1.5)$$

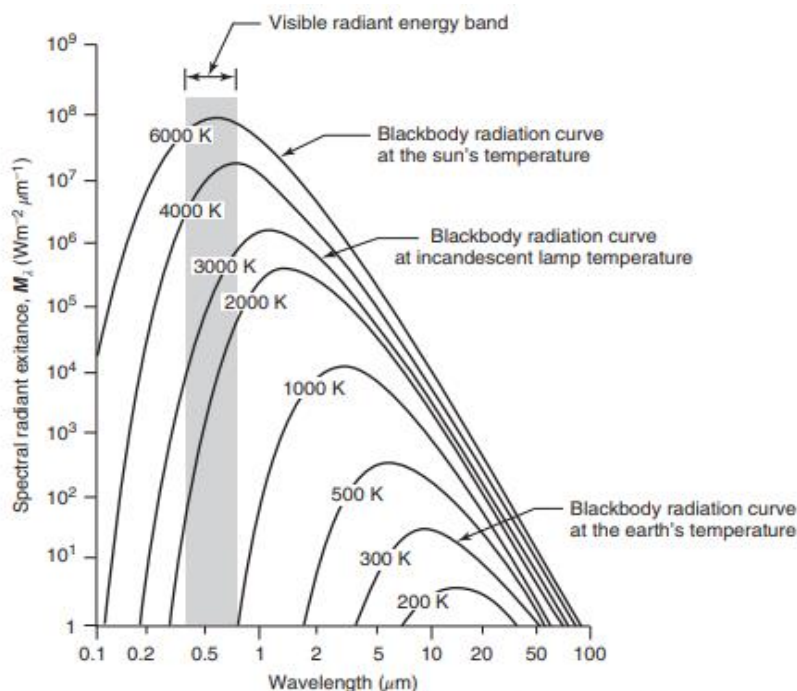
where

$\lambda_m$  = wavelength of maximum spectral radiant exitance,  $\mu\text{m}$

$A$  = 2898  $\mu\text{m K}$

$T$  = temperature, K

Thus, for a blackbody, the wavelength at which the maximum spectral radiant exitance occurs varies inversely with the blackbody’s absolute temperature. We observe this phenomenon when a metal body such as a piece of iron is heated. As the object becomes progressively hotter, it begins to glow and its color changes successively to shorter wavelengths—from dull red to orange to yellow and eventually to white. The sun emits radiation in the same manner as a blackbody radiator whose temperature is about 6000 K (Figure 1.4). Many incandescent lamps emit radiation typified by a 3000 K blackbody radiation curve. Consequently, incandescent lamps have a relatively low output of blue energy, and they do not have the same spectral constituency as sunlight.



**Figure 1.4** Spectral distribution of energy radiated from blackbodies of various temperatures. (Note that spectral radiant exitance  $M_\lambda$  is the energy emitted per unit wavelength interval. Total radiant exitance  $M$  is given by the area under the spectral radiant exitance curves.)



The earth's ambient temperature (i.e., the temperature of surface materials such as soil, water, and vegetation) is about 300 K (27°C). From Wien's displacement law, this means the maximum spectral radiant exitance from earth features occurs at a wavelength of about 9.7  $\mu\text{m}$ . Because this radiation correlates with terrestrial heat, it is termed "thermal infrared" energy. This energy can neither be seen nor photographed, but it can be sensed with such thermal devices as radiometers and. By comparison, the sun has a much higher energy peak that occurs at about 0.5  $\mu\text{m}$ , as indicated in Figure 1.4.

Our eyes—and photographic sensors—are sensitive to energy of this magnitude and wavelength. Thus, when the sun is present, we can observe earth features by virtue of reflected solar energy. Once again, the longer wavelength energy emitted by ambient earth features can be observed only with a nonphotographic sensing system. The general dividing line between reflected and emitted IR wavelengths is approximately 3  $\mu\text{m}$ . Below this wavelength, reflected energy predominates; above it, emitted energy prevails. Certain sensors, such as radar systems, supply their own source of energy to illuminate features of interest. These systems are termed "active" systems, in contrast to "passive" systems that sense naturally available energy. A very common example of an active system is a camera utilizing a flash. The same camera used in sunlight becomes a passive sensor.

# المحاضرة الثانية

CONCEPTS AND FOUNDATIONS OF REMOTE SENSING

### 1.3 ENERGY INTERACTIONS IN THE ATMOSPHERE

Irrespective of its source, all radiation detected by remote sensors passes through some distance, or path length, of atmosphere. The path length involved can vary widely. For example, space photography results from sunlight that passes through the full thickness of the earth's atmosphere twice on its journey from source to sensor. On the other hand, an airborne thermal sensor detects energy emitted directly from objects on the earth, so a single, relatively short atmospheric path length is involved. The net effect of the atmosphere varies with these differences in path length and also varies with the magnitude of the energy signal being sensed, the atmospheric conditions present, and the wavelengths involved. Here, we merely wish to introduce the notion that the atmosphere can have a profound effect on, among other things, the intensity and spectral composition of radiation available to any sensing system. These effects are caused principally through the mechanisms of atmospheric scattering and absorption.

#### Scattering

Atmospheric scattering is the unpredictable diffusion of radiation by particles in the atmosphere. *Rayleigh scatter* is common when radiation interacts with atmospheric molecules and other tiny particles that are much smaller in diameter than the wavelength of the interacting radiation. The effect of Rayleigh scatter is inversely proportional to the fourth power of wavelength. Hence, there is a much stronger tendency for short wavelengths to be scattered by this mechanism than long wavelengths.

A "blue" sky is an indicator of Rayleigh scatter. In the absence of scatter, the sky would appear black. But, as sunlight interacts with the earth's atmosphere, it scatters the shorter (blue) wavelengths more dominantly than the other visible wavelengths. Consequently, we see a blue sky. At sunrise and sunset, however, the sun's rays travel through a longer atmospheric path length than during midday. With the longer path, the scatter (and absorption) of short wavelengths is so complete that we see only the less scattered, longer wavelengths of orange and red. Rayleigh scatter is one of the primary causes of "haze" in imagery. Visually, haze diminishes the "crispness," or "contrast," of an image. In color photography, it results in a bluish-gray cast to an image, particularly when taken from high altitude. Haze can often be eliminated or at least minimized by introducing, in front of the camera lens, a filter that does not transmit short wavelengths.

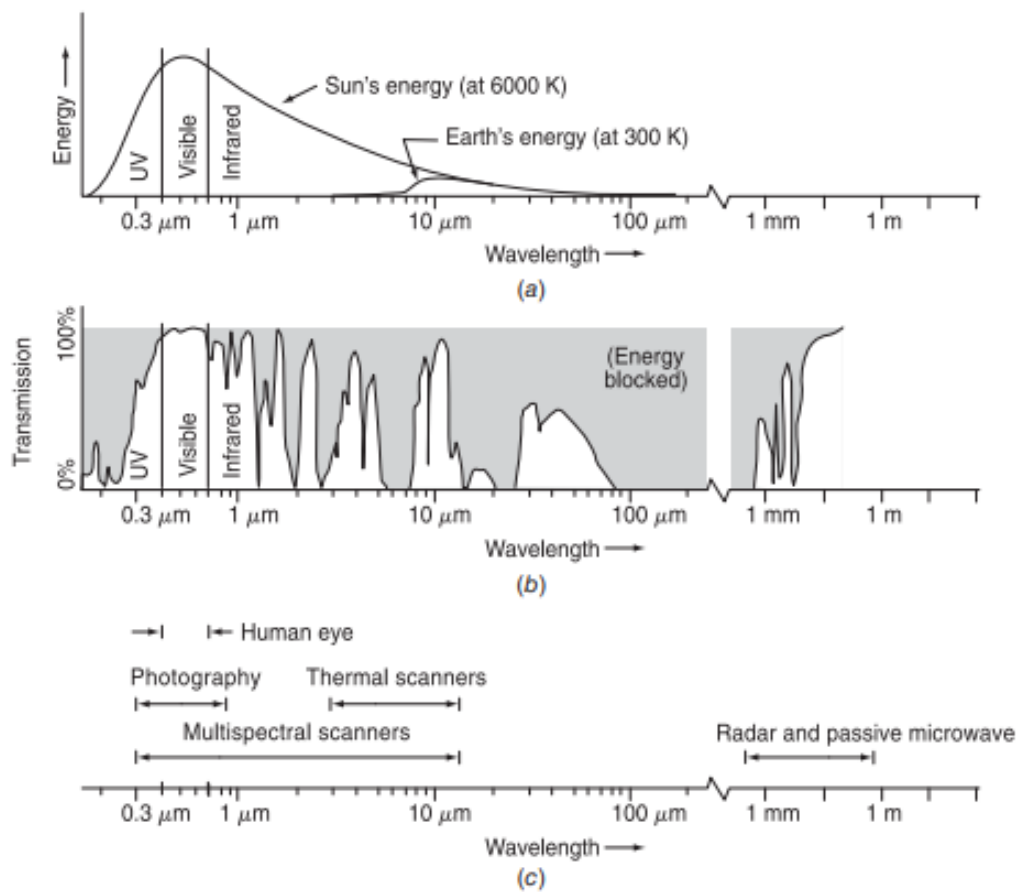
Another type of scatter is *Mie scatter*, which exists when atmospheric particle diameters essentially equal the wavelengths of the energy being sensed. Water vapor and dust are major causes of Mie scatter. This type of scatter tends to influence longer wavelengths compared to Rayleigh scatter. Although Rayleigh scatter tends to dominate under most atmospheric conditions, Mie scatter is significant in slightly overcast ones.

A more bothersome phenomenon is *nonselective scatter*, which comes about when the diameters of the particles causing scatter are much larger than the wavelengths of the energy being sensed. Water droplets, for example, cause such scatter. They commonly have a diameter in the range 5 to 100<sup>m</sup> m and scatter all visible and near- to mid-IR wavelengths about equally. Consequently, this scattering is "nonselective" with respect to wavelength. In the visible wavelengths, equal quantities of blue, green, and red light are scattered; hence fog and clouds appear white.

#### Absorption

In contrast to scatter, atmospheric absorption results in the effective loss of energy to atmospheric constituents. This normally involves absorption of energy at a given wavelength. The most efficient

absorbers of solar radiation in this regard are water vapor, carbon dioxide, and ozone. Because these gases tend to absorb electromagnetic energy in specific wavelength bands, they strongly influence the design of any remote sensing system. The wavelength ranges in which the atmosphere is particularly transmissive of energy are referred to as atmospheric windows. Figure 1.5 shows the interrelationship between energy sources and atmospheric absorption characteristics. Figure 1.5a shows the spectral distribution of the energy emitted by the sun and by earth features. These two curves represent the most common sources of energy used in remote sensing. In Figure 1.5b, spectral regions in which the atmosphere blocks energy are shaded. Remote sensing data acquisition is limited to the nonblocked spectral regions, the atmospheric windows. Note in Figure 1.5c that the spectral sensitivity range of the eye (the “visible” range) coincides with both an atmospheric window and the peak level of energy from the sun. Emitted “heat” energy from the earth, shown by the small curve in (a), is sensed through the windows at 3 to 5  $\mu\text{m}$  and 8 to 14  $\mu\text{m}$  using such devices as thermal sensors. Multispectral sensors observe simultaneously through multiple, narrow wavelength ranges that can be located at various points in the visible through the thermal spectral region. Radar and passive microwave systems operate through a window in the region 1 mm to 1 m. The important point to note from Figure 1.5 is the interaction and the interdependence between the primary sources of electromagnetic energy, the atmospheric windows through which source energy may be transmitted to and from earth surface features, and the spectral sensitivity of the sensors available to detect and record the energy. One cannot select the sensor to be used in any given remote sensing task arbitrarily; one must instead consider (1) the spectral sensitivity of the sensors available, (2) the presence or absence of atmospheric windows in the spectral range(s) in which one wishes to sense, and (3) the source, magnitude, and spectral composition of the energy available in these ranges. Ultimately, however, the choice of spectral range of the sensor must be based on the manner in which the energy interacts with the features under investigation. It is to this last, very important, element that we now turn our attention.



**Figure 1.5** Spectral characteristics of (a) energy sources, (b) atmospheric transmittance, and (c) common remote sensing systems. (Note that wavelength scale is logarithmic.)

# المحاضرة

## الثالثة

CONCEPTS AND FOUNDATIONS OF REMOTE SENSING

## 1.4 ENERGY INTERACTIONS WITH EARTH SURFACE FEATURES

When electromagnetic energy is incident on any given earth surface feature, three fundamental energy interactions with the feature are possible. These are illustrated in Figure 1.6 for an element of the volume of a water body. Various fractions of the energy incident on the element are reflected, absorbed, and/or transmitted. Applying the principle of conservation of energy, we can state the interrelationship among these three energy interactions as

$$E_I(\lambda) = E_R(\lambda) + E_A(\lambda) + E_T(\lambda) \quad (1.6)$$

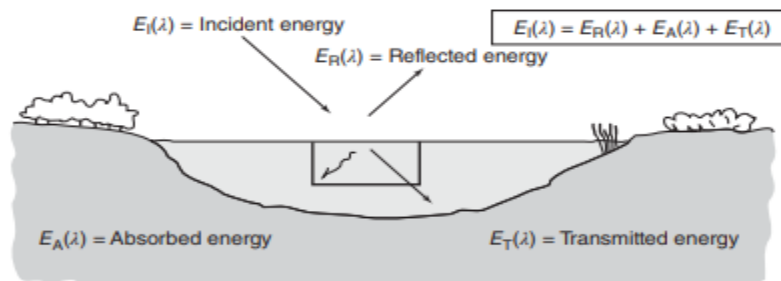
where

- $E_I$  = incident energy
- $E_R$  = reflected energy
- $E_A$  = absorbed energy
- $E_T$  = transmitted energy

with all energy components being a function of wavelength  $\lambda$ .

Equation 1.6 is an energy balance equation expressing the interrelationship among the mechanisms of reflection, absorption, and transmission. Two points concerning this relationship should be noted. First, the proportions of energy reflected, absorbed, and transmitted will vary for different earth features, depending on their material type and condition. These differences permit us to distinguish different features on an image. Second, the wavelength dependency means that, even within a given feature type, the proportion of reflected, absorbed, and transmitted energy will vary at different wavelengths. Thus, two features may be indistinguishable in one spectral range and be very different in another wavelength band. Within the visible portion of the spectrum, these spectral variations result in the visual effect called color. For example, we call objects “blue” when they reflect more highly in the blue portion of the spectrum, “green” when they reflect more highly in the green spectral region, and so on. Thus, the eye utilizes spectral variations in the magnitude of reflected energy to discriminate between various objects. Because many remote sensing systems operate in the wavelength regions in which reflected energy predominates, the reflectance properties of earth features are very important. Hence, it is often useful to think of the energy balance relationship expressed by Eq. 1.6 in the form

$$E_R(\lambda) = E_I(\lambda) - [E_A(\lambda) + E_T(\lambda)] \quad (1.7)$$



**Figure 1.6** Basic interactions between electromagnetic energy and an earth surface feature.

That is, the reflected energy is equal to the energy incident on a given feature reduced by the energy that is either absorbed or transmitted by that feature. The reflectance characteristics of earth surface features may be quantified by measuring the portion of incident energy that is reflected. This is measured as a function of wavelength and is called spectral reflectance,  $\rho_\lambda$ . It is mathematically defined as

$$\rho_\lambda = \frac{E_R(\lambda)}{E_I(\lambda)}$$

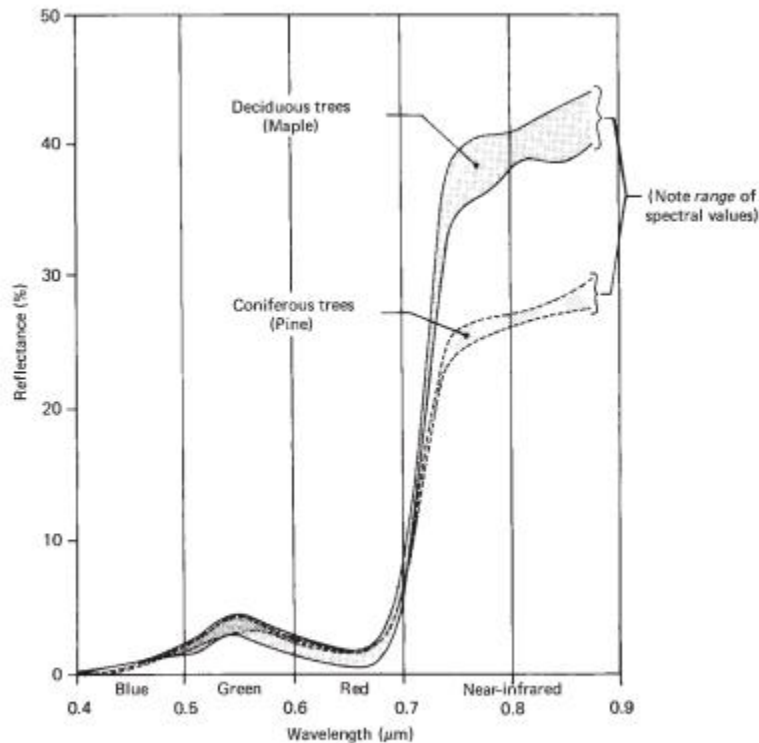
$$= \frac{\text{energy of wavelength } \lambda \text{ reflected from the object}}{\text{energy of wavelength } \lambda \text{ incident upon the object}} \times 100 \quad (1.8)$$

where  $\rho_\lambda$  is expressed as a percentage.

A graph of the spectral reflectance of an object as a function of wavelength is termed a spectral reflectance curve. The configuration of spectral reflectance curves gives us insight into the spectral characteristics of an object and has a strong influence on the choice of wavelength region(s) in which remote sensing data are acquired for a particular application. This is illustrated in Figure 1.7, which shows highly generalized spectral reflectance curves for deciduous versus coniferous trees. Note that the curve for each of these object types is plotted as a “ribbon” (or “envelope”) of values, not as a single line. This is because spectral reflectances vary somewhat within a given material class. That is, the spectral reflectance of one deciduous tree species and another will never be identical, nor will the spectral reflectance of trees of the same species be exactly equal. We elaborate upon the variability of spectral reflectance curves later in this section. In Figure 1.7, assume that you are given the task of selecting an airborne sensor system to assist in preparing a map of a forested area differentiating deciduous versus coniferous trees. One choice of sensor might be the human eye. However, there is a potential problem with this choice. The spectral reflectance curves for each tree type overlap in most of the visible portion of the spectrum and are very close where they do not overlap. Hence, the eye might see both tree types as being essentially the same shade of “green” and might confuse the identity of the deciduous and coniferous trees. Certainly one could improve things somewhat by using spatial clues to each tree type’s identity, such as size, shape, site, and so forth. However, this is often difficult to do from the air, particularly when tree types are intermixed. How might we discriminate the two types on the basis of their spectral characteristics alone? We could do this by using a sensor that records near-IR energy. A specialized digital camera whose detectors are sensitive to near-IR wavelengths is just such a system, as is an analog camera loaded with black and white IR film. On near-IR images, deciduous trees (having higher IR reflectance than conifers) generally appear much lighter in tone than do conifers.

On such an image, the task of delineating deciduous versus coniferous trees becomes almost trivial. In fact, if we were to use a computer to analyze digital data collected from this type of sensor, we might “automate” our entire mapping task. Many remote sensing data analysis schemes attempt to do just that. For these schemes to be successful, the materials to be differentiated must be spectrally separable. Experience has shown that many earth surface features of interest can be identified, mapped, and studied on the basis of their spectral characteristics. Experience has also shown that some features of interest cannot be spectrally separated. Thus, to utilize remote sensing data effectively, one must know and understand the spectral characteristics of the particular features under investigation in any given application. Likewise, one must know what factors influence these characteristics.





**Figure 1.7** Generalized spectral reflectance envelopes for deciduous (broad-leaved) and coniferous (needle-bearing) trees. (Each tree type has a range of spectral reflectance values at any wavelength.) (Adapted from Kalensky and Wilson, 1975.)

### Spectral Reflectance of Earth Surface Feature Types.

Figure 1.9 shows typical spectral reflectance curves for many different types of features: healthy green grass, dry (non-photosynthetically active) grass, bare soil (brown to dark-brown sandy loam), pure gypsum dune sand, asphalt, construction concrete (Portland cement concrete), fine-grained snow, clouds, and clear lake water. The lines in this figure represent average reflectance curves compiled by measuring a large sample of features, or in some cases representative reflectance measurements from a single typical example of the feature class. Note how distinctive the curves are for each feature. In general, the configuration of these curves is an indicator of the type and condition of the features to which they apply. Although the reflectance of individual features can vary considerably above and below the lines shown here, these curves demonstrate some fundamental points concerning spectral reflectance. For example, spectral reflectance curves for healthy green vegetation almost always manifest the “peak-and-valley” configuration illustrated by green grass in Figure 1.9. The valleys in the visible portion of the spectrum are dictated by the pigments in plant leaves. Chlorophyll, for example, strongly absorbs energy in the wavelength bands centered at about 0.45 and 0.67  $\mu\text{m}$  (often called the “chlorophyll absorption bands”). Hence, our eyes perceive healthy vegetation as green in color because of the very high absorption of blue and red energy by plant leaves and the relatively high reflection of green energy. If a plant is subject to some form of stress that interrupts its normal growth and productivity, it may decrease or cease chlorophyll production. The result is less chlorophyll absorption in the blue and red bands. Often, the red reflectance increases to the point that we see the plant turn yellow (combination of green and red). This can be seen in the spectral curve for dried grass in Figure 1.9.

As we go from the visible to the near-IR portion of the spectrum, the reflectance of healthy vegetation increases dramatically. This spectral feature, known as the red edge, typically occurs between 0.68 and 0.75  $\mu\text{m}$ , with the exact position depending on the species and condition. Beyond this edge, from about 0.75 to 1.3  $\mu\text{m}$  (representing most of the near-IR range), a plant leaf typically reflects 40 to 50% of the energy incident upon it. Most of the remaining energy is transmitted, because absorption in this spectral region is minimal (less than 5%). Plant reflectance from 0.75 to 1.3  $\mu\text{m}$  results primarily from the internal structure of plant leaves. Because the position of the red edge and the magnitude of the near-IR reflectance beyond the red edge are highly variable among plant species, reflectance measurements in these ranges often permit us to discriminate between species, even if they look the same in visible wavelengths. Likewise, many plant stresses alter the reflectance in the red edge and the near-IR region, and sensors operating in these ranges are often used for vegetation stress detection. Also, multiple layers of leaves in a plant canopy provide the opportunity for multiple transmissions and reflections. Hence, the near-IR reflectance increases with the number of layers of leaves in a canopy, with the maximum reflectance achieved at about eight leaf layers (Bauer et al., 1986).

Beyond 1.3  $\mu\text{m}$ , energy incident upon vegetation is essentially absorbed or reflected, with little to no transmittance of energy. Dips in reflectance occur at 1.4, 1.9, and 2.7  $\mu\text{m}$  because water in the leaf absorbs strongly at these wavelengths. Accordingly, wavelengths in these spectral regions are referred to as water absorption bands. Reflectance peaks occur at about 1.6 and 2.2  $\mu\text{m}$ , between the absorption bands. Throughout the range beyond 1.3  $\mu\text{m}$ , leaf reflectance is approximately inversely related to the total water present in a leaf. This total is a function of both the moisture content and the thickness of a leaf.

The soil curve in Figure 1.9 shows considerably less peak-and-valley variation in reflectance. That is, the factors that influence soil reflectance act over less specific spectral bands. Some of the factors affecting soil reflectance are moisture content, organic matter content, soil texture (proportion of sand, silt, and clay), surface roughness, and presence of iron oxide. These factors are complex, variable, and interrelated. For example, the presence of moisture in soil will decrease its reflectance. As with vegetation, this effect is greatest in the water absorption bands at about 1.4, 1.9, and 2.7  $\mu\text{m}$  (clay soils also have hydroxyl absorption bands at about 1.4 and 2:2  $\mu\text{m}$ ). Soil moisture content is strongly related to the soil texture: Coarse, sandy soils are usually well drained, resulting in low moisture content and relatively high reflectance; poorly drained fine-textured soils will generally have lower reflectance. Thus, the reflectance properties of a soil are consistent only within particular ranges of conditions. Two other factors that reduce soil reflectance are surface roughness and content of organic matter. The presence of iron oxide in a soil will also significantly decrease reflectance, at least in the visible wavelengths. In any case, it is essential that the analyst be familiar with the conditions at hand. Finally, because soils are essentially opaque to visible and infrared radiation, it should be noted that soil reflectance comes from the uppermost layer of the soil and may not be indicative of the properties of the bulk of the soil.

Sand can have wide variation in its spectral reflectance pattern. The curve shown in Figure 1.9 is from a dune in New Mexico and consists of roughly 99% gypsum with trace amounts of quartz (Jet Propulsion Laboratory, 1999). Its absorption and reflectance features are essentially identical to those of its parent material, gypsum. Sand derived from other sources, with differing mineral compositions, would have a spectral reflectance curve indicative of its parent material. Other factors affecting the spectral response from sand include the presence or absence of water and of organic matter. Sandy soil is subject to the same considerations listed in the discussion of soil reflectance.

As shown in Figure 1.9, the spectral reflectance curves for asphalt and Portland cement concrete are much flatter than those of the materials discussed thus far. Overall, Portland cement concrete tends to be relatively brighter than asphalt, both in the visible spectrum and at longer wavelengths. It is important to

note that the reflectance of these materials may be modified by the presence of paint, soot, water, or other substances. Also, as materials age, their spectral reflectance patterns may change. For example, the reflectance of many types of asphaltic concrete may increase, particularly in the visible spectrum, as their surface ages.

In general, snow reflects strongly in the visible and near infrared, and absorbs more energy at mid-infrared wavelengths. However, the reflectance of snow is affected by its grain size, liquid water content, and presence or absence of other materials in or on the snow surface (Dozier and Painter, 2004). Larger grains of snow absorb more energy, particularly at wavelengths longer than 0.8  $\mu\text{m}$ . At temperatures near 0°C, liquid water within the snowpack can cause grains to stick together in clusters, thus increasing the effective grain size and decreasing the reflectance at near-infrared and longer wavelengths. When particles of contaminants such as dust or soot are deposited on snow, they can significantly reduce the surface's reflectance in the visible spectrum.

The aforementioned absorption of mid-infrared wavelengths by snow can permit the differentiation between snow and clouds. While both feature types appear bright in the visible and near infrared, clouds have significantly higher reflectance than snow at wavelengths longer than 1.4  $\mu\text{m}$ . Meteorologists can also use both spectral and bidirectional reflectance patterns (discussed later in this section) to identify a variety of cloud properties, including ice/water composition and particle size.

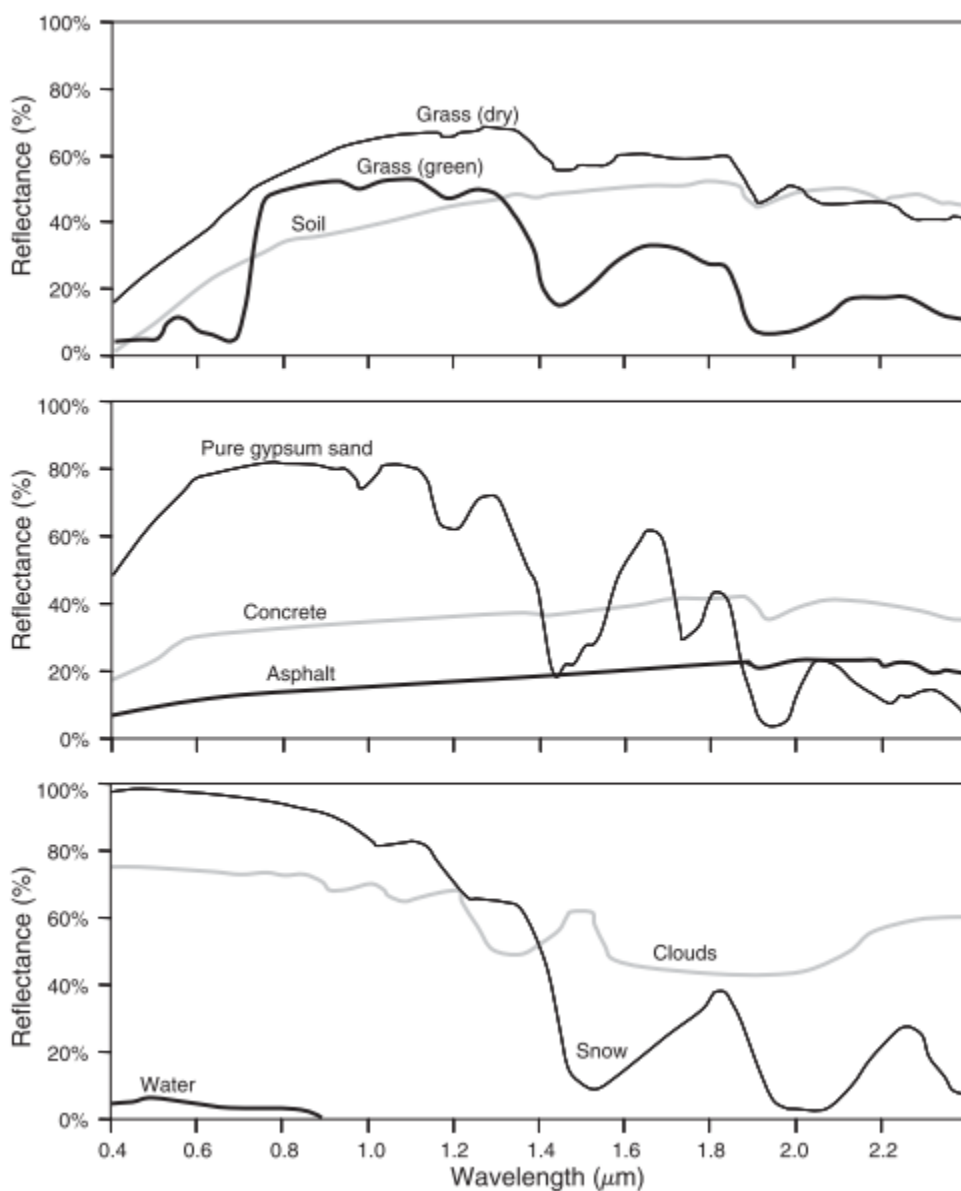
Considering the spectral reflectance of water, probably the most distinctive characteristic is the energy absorption at near-IR wavelengths and beyond. In short, water absorbs energy in these wavelengths whether we are talking about water features per se (such as lakes and streams) or water contained in vegetation or soil. Locating and delineating water bodies with remote sensing data are done most easily in near-IR wavelengths because of this absorption property. However, various conditions of water bodies manifest themselves primarily in visible wavelengths. The energy-matter interactions at these wavelengths are very complex and depend on a number of interrelated factors. For example, the reflectance from a water body can stem from an interaction with the water's surface (specular reflection), with material suspended in the water, or with the bottom of the depression containing the water body. Even with deep water where bottom effects are negligible, the reflectance properties of a water body are a function of not only the water per se but also the material in the water.

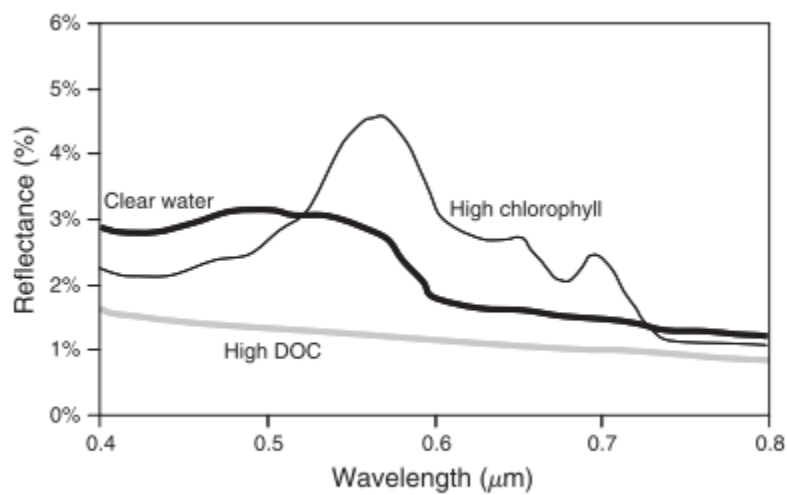
Clear water absorbs relatively little energy having wavelengths less than about 0.6  $\mu\text{m}$ . High transmittance typifies these wavelengths with a maximum in the blue-green portion of the spectrum. However, as the turbidity of water changes (because of the presence of organic or inorganic materials), transmittance—and therefore reflectance—changes dramatically. For example, waters containing large quantities of suspended sediments resulting from soil erosion normally have much higher visible reflectance than other “clear” waters in the same geographic area. Likewise, the reflectance of water changes with the chlorophyll concentration involved. Increases in chlorophyll concentration tend to decrease water reflectance in blue wavelengths and increase it in green wavelengths. These changes have been used to monitor the presence and estimate the concentration of algae via remote sensing data. Reflectance data have also been used to determine the presence or absence of tannin dyes from bog vegetation in lowland areas and to detect a number of pollutants, such as oil and certain industrial wastes.

Figure 1.10 illustrates some of these effects, using spectra from three lakes with different bio-optical properties. The first spectrum is from a clear, oligotrophic lake with a chlorophyll level of 1:2  $\mu\text{g/l}$  and only 2.4 mg/l of dissolved organic carbon (DOC). Its spectral reflectance is relatively high in the blue-green portion of the spectrum and decreases in the red and near infrared. In contrast, the spectrum from a lake experiencing an algae bloom, with much higher chlorophyll concentration 12.3  $\mu\text{g/l}$ , shows a

reflectance peak in the green spectrum and absorption in the blue and red regions. These reflectance and absorption features are associated with several pigments present in algae. Finally, the third spectrum in Figure 1.10 was acquired on an ombrotrophic bog lake, with very high levels of DOC (20.7 mg/l). These naturally occurring tannins and other complex organic molecules give the lake a very dark appearance, with its reflectance curve nearly flat across the visible spectrum.

Many important water characteristics, such as dissolved oxygen concentration, pH, and salt concentration, cannot be observed directly through changes in water reflectance. However, such parameters sometimes correlate with observed reflectance. In short, there are many complex interrelationships between the spectral reflectance of water and particular characteristics. One must use appropriate reference data to correctly interpret reflectance measurements made over water.





**Figure 1.10** Spectral reflectance curves for lakes with clear water, high levels of chlorophyll, and high levels of dissolved organic carbon (DOC).

# المحاضرة الرابعة

*CONCEPTS AND FOUNDATIONS OF REMOTE SENSING*

### ***Spectral Response Patterns***

Having looked at the spectral reflectance characteristics of vegetation, soil, sand, concrete, asphalt, snow, clouds, and water, we should recognize that these broad feature types are often spectrally separable. However, the degree of separation between types varies among and within spectral regions. For example, water and vegetation might reflect nearly equally in visible wavelengths, yet these features are almost always separable in near-IR wavelengths.

Because spectral responses measured by remote sensors over various features often permit an assessment of the type and/or condition of the features, these responses have often been referred to as spectral signatures. Spectral reflectance and spectral emittance curves (for wavelengths greater than 3.0  $\mu\text{m}$ ) are often referred to in this manner. The physical radiation measurements acquired over specific terrain features at various wavelengths are also referred to as the spectral signatures for those features.

Although it is true that many earth surface features manifest very distinctive spectral reflectance and/or emittance characteristics, these characteristics result in spectral “response patterns” rather than in spectral “signatures.” The reason for this is that the term signature tends to imply a pattern that is absolute and unique. This is not the case with the spectral patterns observed in the natural world. As we have seen, spectral response patterns measured by remote sensors may be quantitative, but they are not absolute. They may be distinctive, but they are not necessarily unique.

We have already looked at some characteristics of objects that influence their spectral response patterns. Temporal effects and spatial effects can also enter into any given analysis. Temporal effects are any factors that change the spectral characteristics of a feature over time. For example, the spectral characteristics of many species of vegetation are in a nearly continual state of change throughout a growing season. These changes often influence when we might collect sensor data for a particular application.

Spatial effects refer to factors that cause the same types of features (e.g., corn plants) at a given point in time to have different characteristics at different geographic locations. In small-area analysis the geographic locations may be meters apart and spatial effects may be negligible. When analyzing satellite data, the locations may be hundreds of kilometers apart where entirely different soils, climates, and cultivation practices might exist.

Temporal and spatial effects influence virtually all remote sensing operations. These effects normally complicate the issue of analyzing spectral reflectance properties of earth resources. Again, however, temporal and spatial effects might be the keys to gleaning the information sought in an analysis. For example, the process of change detection is premised on the ability to measure temporal effects. An example of this process is detecting the change in suburban development near a metropolitan area by using data obtained on two different dates.

### ***Atmospheric Influences on Spectral Response Patterns***

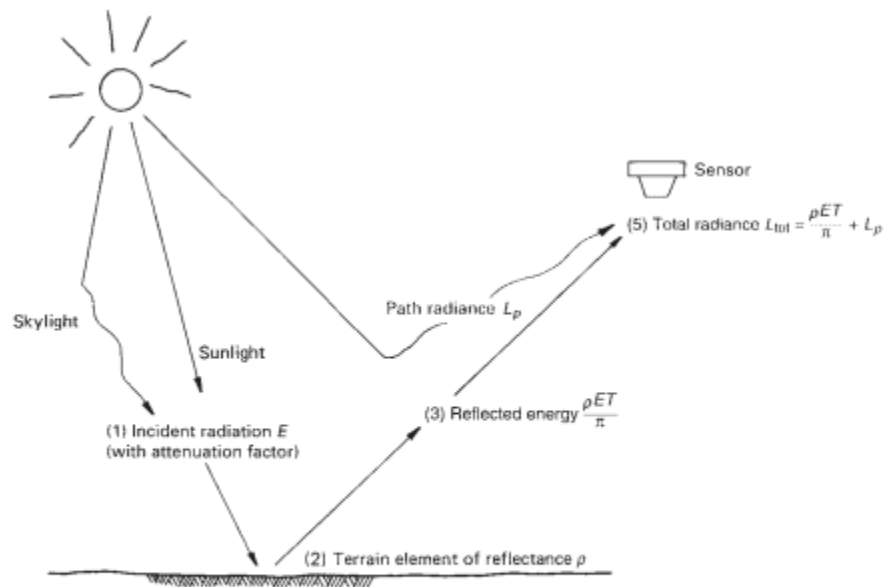
In addition to being influenced by temporal and spatial effects, spectral response patterns are influenced by the atmosphere. Regrettably, the energy recorded by a sensor is always modified to some extent by the atmosphere between the sensor and the ground. Figure 1.11 provides an initial frame of reference for understanding the nature of atmospheric effects. Shown in this figure is the typical situation encountered when a sensor records reflected solar energy. The atmosphere affects the “brightness,” or radiance, recorded over any given point on the ground in two almost contradictory ways. First, it attenuates

(reduces) the energy illuminating a ground object (and being reflected from the object). Second, the atmosphere acts as a reflector itself, adding a scattered, extraneous path radiance to the signal detected by the sensor. By expressing these two atmospheric effects mathematically, the total radiance recorded by the sensor may be related to the reflectance of the ground object and the incoming radiation or irradiance using the equation

$$L_{\text{tot}} = \frac{\rho ET}{\pi} + L_p \quad (1.9)$$

where

- $L_{\text{tot}}$  = total spectral radiance measured by sensor
- $\rho$  = reflectance of object
- $E$  = irradiance on object, incoming energy
- $T$  = transmission of atmosphere
- $L_p$  = path radiance, from the atmosphere and not from the object

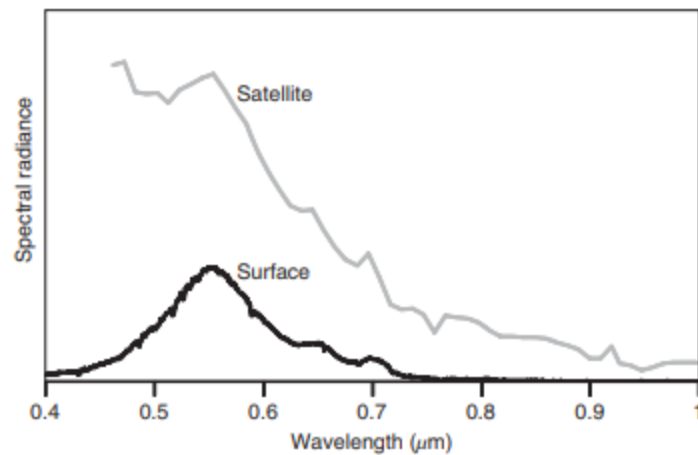


**Figure 1.11** Atmospheric effects influencing the measurement of reflected solar energy. Attenuated sunlight and skylight ( $E$ ) is reflected from a terrain element having reflectance  $\rho$ . The attenuated radiance reflected from the terrain element ( $\rho ET/\pi$ ) combines with the path radiance ( $L_p$ ) to form the total radiance ( $L_{\text{tot}}$ ) recorded by the sensor.

It should be noted that all of the above factors depend on wavelength. Also, as shown in Figure 1.11, the irradiance ( $E$ ) stems from two sources: (1) directly reflected “sunlight” and (2) diffuse “skylight,” which is sunlight that has been previously scattered by the atmosphere. The relative dominance of sunlight versus skylight in any given image is strongly dependent on weather conditions (e.g., sunny vs. hazy vs. cloudy). Likewise, irradiance varies with the seasonal changes in solar elevation angle (Figure 7.4) and the changing distance between the earth and sun.



For a sensor positioned close to the earth's surface, the path radiance  $L_p$  will generally be small or negligible, because the atmospheric path length from the surface to the sensor is too short for much scattering to occur. In contrast, imagery from satellite systems will be more strongly affected by path radiance, due to the longer atmospheric path between the earth's surface and the spacecraft. This can be seen in Figure 1.12, which compares two spectral response patterns from the same area. One "signature" in this figure was collected using a handheld field spectroradiometer (see Section 1.6 for discussion), from a distance of only a few cm above the surface. The second curve shown in Figure 1.12 was collected by the Hyperion hyperspectral sensor on the EO-1 satellite (hyperspectral systems



**Figure 1.12** Spectral response patterns measured using a field spectroradiometer in close proximity to the earth's surface, and from above the top of the atmosphere (via the Hyperion instrument on EO-1). The difference between the two "signatures" is caused by atmospheric scattering and absorption in the Hyperion image.

# المحاضرة الخامسة

**Basic Principles of Photogrammetry**

## Chapter two

**Basic Principles of Photogrammetry****1.2 INTRODUCTION**

*Photogrammetry* is the science and technology of obtaining spatial measurements and other geometrically reliable derived products from photographs. Historically, photogrammetric analyses involved the use of hardcopy photographic products such as paper prints or film transparencies. Today, most photogrammetric procedures involve the use of digital, or softcopy, photographic data products. In certain cases, these digital products might result from high resolution scanning of hardcopy photographs (e.g., historical photographs). However, the overwhelming majority of digital photographs used in modern photogrammetric applications come directly from digital cameras. In fact, photogrammetric processing of digital camera data is often accomplished in-flight such that digital orthophotos, digital elevation models (DEMs), and other GIS data products are available immediately after, or even during, an aerial photographic mission.

While the physical character of hardcopy and digital photographs is quite different, the basic geometric principles used to analyze them photogrammetrically are identical. In fact, it is often easier to visualize and understand these principles in a hardcopy context and then extend them to the softcopy environment. This is the approach we adopt in this chapter. Hence, our objective in this discussion is to not only prepare the reader to be able to make basic measurements from hardcopy photographic images, but also to understand the underlying principles of modern digital (softcopy) photogrammetry. We stress aerial photogrammetric techniques and procedures in this discussion, but the same general principles hold for terrestrial (ground-based) and space-based operations as well.

In this chapter, we introduce only the most basic aspects of the broad subject of photogrammetry. (More comprehensive and detailed treatment of the subject of photogrammetry is available in such references as ASPRS, 2004; Mikhail et al., 2001; and Wolf et al., 2013.) We limit our discussion to the following photogrammetric activities:

1. **Determining the scale of a vertical photograph and estimating horizontal ground distances from measurements made on a vertical photograph.** The scale of a photograph expresses the mathematical relationship between a distance measured on the photo and the corresponding horizontal distance measured in a ground coordinate system. Unlike maps, which have a single constant scale, aerial photographs have a range of scales that vary in proportion to the elevation of the terrain involved. Once the scale of a photograph is known at any particular elevation, ground distances at that elevation can be readily estimated from corresponding photo distance measurements.
2. **Using area measurements made on a vertical photograph to determine the equivalent areas in a ground coordinate system.** Computing ground areas from corresponding photo area measurement is simply an extension of the above concept of scale. The only difference is that whereas ground distances and photo distances vary linearly, ground areas and photo areas vary as the square of the scale.
3. **Quantifying the effects of relief displacement on vertical aerial photographs.** Again unlike maps, aerial photographs in general do not show the true plan or top view of objects. The images of the tops of objects appearing in a photograph are displaced from the images of their bases. This is known as relief displacement and causes any object standing above the terrain to “lean

away” from the principal point of a photograph radially. Relief displacement, like scale variation, precludes the use of aerial photographs directly as maps. However, reliable ground measurements and maps can be obtained from vertical photographs if photo measurements are analyzed with due regard for scale variations and relief displacement.

4. **Determining object heights from relief displacement measurements.** While relief displacement is usually thought of as an image distortion that must be dealt with, it can also be used to estimate the heights of objects appearing on a photograph. As we later illustrate, the magnitude of relief displacement depends on the flying height, the distance from the photo principal point to the feature, and the height of the feature. Because these factors are geometrically related, we can measure an object’s relief displacement and radial position on a photograph and thereby determine the height of the object. This technique provides limited accuracy but is useful in applications where only approximate object heights are needed.
5. **Determining object heights and terrain elevations by measuring image parallax.** The previous operations are performed using vertical photos individually. Many photogrammetric operations involve analyzing images in the area of overlap of a stereopair. Within this area, we have two views of the same terrain, taken from different vantage points. Between these two views, the relative positions of features lying closer to the camera (at higher elevation) will change more from photo to photo than the positions of features farther from the camera (at lower elevation). This change in relative position is called parallax. It can be measured on overlapping photographs and used to determine object heights and terrain elevations.
6. **Determining the elements of exterior orientation of aerial photographs.** In order to use aerial photographs for photogrammetric mapping purposes, it is necessary to determine six independent parameters that describe the position and angular orientation of each photograph at the instant of its exposure relative to the origin and orientation of the ground coordinate system used for mapping. These six variables are called the elements of exterior orientation. Three of these are the 3D position ( $X, Y, Z$ ) of the center of the photocoordinate axis system at the instant of exposure. The remaining three are the 3D rotation angles  $(\omega, \phi, \kappa)$  related to the amount and direction of tilt in each photo at the instant of exposure. These rotations are a function of the orientation of the platform and camera mount when the photograph is taken. For example, the wings of a fixed-wing aircraft might be tilted up or down, relative to horizontal. Simultaneously, the camera might be tilted up or down toward the front or rear of the aircraft. At the same time, the aircraft might be rotated into a headwind in order to maintain a constant heading. We will see that there are two major approaches that can be taken to determine the elements of exterior orientation. The first involves the use of ground control (photo-identifiable points of known ground coordinates) together with a mathematical procedure called aerotriangulation. The second approach entails direct georeferencing, which involves the integration of GPS and IMU observations to determine the position and angular orientation of each photograph. We treat both of these approaches at a conceptual level, with a minimum of mathematical detail.
7. **Production of maps, DEMs, and orthophotos.** “Mapping” from aerial photographs can take on many forms. Historically, topographic maps were produced using hardcopy stereopairs placed in a device called a stereoplotter. With this type of instrument the photographs are mounted in special projectors that can be mutually oriented to precisely correspond to the angular tilts  $(\omega, \phi, \kappa)$  present when the photographs were taken. Each of the projectors can also be translated in  $x, y,$  and  $z$  such that a reduced-size model is created that exactly replicates the exterior orientation of each of the photographs comprising the stereopair. (The scale of the resulting

stereomodel is determined by the “air base” distance between the projectors chosen by the instrument operator.) When viewed stereoscopically, the model can be used to prepare an analog or digital planimetric map having no tilt or relief distortions. In addition, topographic contours can be integrated with the planimetric data and the height of individual features appearing in the model can be determined.

8. **Preparing a flight plan to acquire vertical aerial photography.** Whenever new photographic coverage of a project area is to be obtained, a photographic flight mission must be planned. As we will discuss, mission planning software highly automates this process. However, most readers of this book are, or will become, consumers of image data rather than providers. Such individuals likely will not have direct access to flight planning software and will appropriately rely on professional data suppliers to jointly design a mission to meet their needs. There are also cases where cost and logistics might dictate that the data consumer and the data provider are one in the same.

## 2.2 BASIC GEOMETRIC CHARACTERISTICS OF AERIAL PHOTOGRAPHS

### Geometric Types of Aerial Photographs

Aerial photographs are generally classified as either vertical or oblique. Vertical photographs are those made with the camera axis directed as vertically as possible. However, a “truly” vertical aerial photograph is rarely obtainable because of the previously described unavoidable angular rotations, or tilts, caused by the angular attitude of the aircraft at the instant of exposure. These unavoidable tilts cause slight ( $1^\circ$  to  $3^\circ$ ) unintentional inclination of the camera optical axis, resulting in the acquisition of tilted photographs.

Virtually all photographs are tilted. When tilted unintentionally and slightly, tilted photographs can be analyzed using the simplified models and methods appropriate to the analysis of truly vertical photographs without the introduction of serious error. This is done in many practical applications where approximate measurements suffice (e.g., determining the ground dimensions of a flat agricultural field based on photo measurements made with a scale or digitizing tablet). However, as we will discuss, precise digital photogrammetric procedures employ methods and models that rigorously account for even very small angles of tilt with no loss of accuracy.

When aerial photographs are taken with an intentional inclination of the camera axis, oblique photographs result. High oblique photographs include an image of the horizon, and low oblique photographs do not. In this chapter, we emphasize the geometric aspects of acquiring and analyzing vertical aerial photographs given their extensive historical and continuing use for large-area photogrammetric mapping. However, the use of oblique aerial photographs has increased rapidly in such applications as urban mapping and disaster assessment. With their “side-view” character, oblique photographs afford a more natural perspective in comparison to the top view perspective of vertical aerial photographs. This can greatly facilitate the image interpretation process (particularly for those individuals having limited training or experience in image interpretation). Various examples of oblique aerial photographs are interspersed throughout this book.

Photogrammetric measurements can also be made from oblique aerial photographs if they are acquired with this purpose in mind. This is often accomplished using multiple cameras that are shuttered simultaneously.

### Taking Vertical Aerial Photographs

Most vertical aerial photographs are taken with frame cameras along flight lines, or flight strips. The line traced on the ground directly beneath the aircraft during acquisition of photography is called the nadir line. This line connects the image centers of the vertical photographs. Figure 2.1 illustrates the typical character of the photographic coverage along a flight line. Successive photographs are generally taken with some degree of endlap. Not only does this lapping ensure total coverage along a flight line, but an endlap of at least 50% is essential for total stereoscopic coverage of a project area. Stereoscopic coverage consists of adjacent pairs of overlapping vertical photographs called stereopairs. Stereopairs provide two different perspectives of the ground area in their region of endlap. When images forming a stereopair are viewed through a stereoscope, each eye psychologically occupies the vantage point from which the respective image of the stereopair was taken in flight. The result is the perception of a three-dimensional stereomodel. Most applications of aerial photographic interpretation entail the use of stereoscopic coverage and stereoviewing.

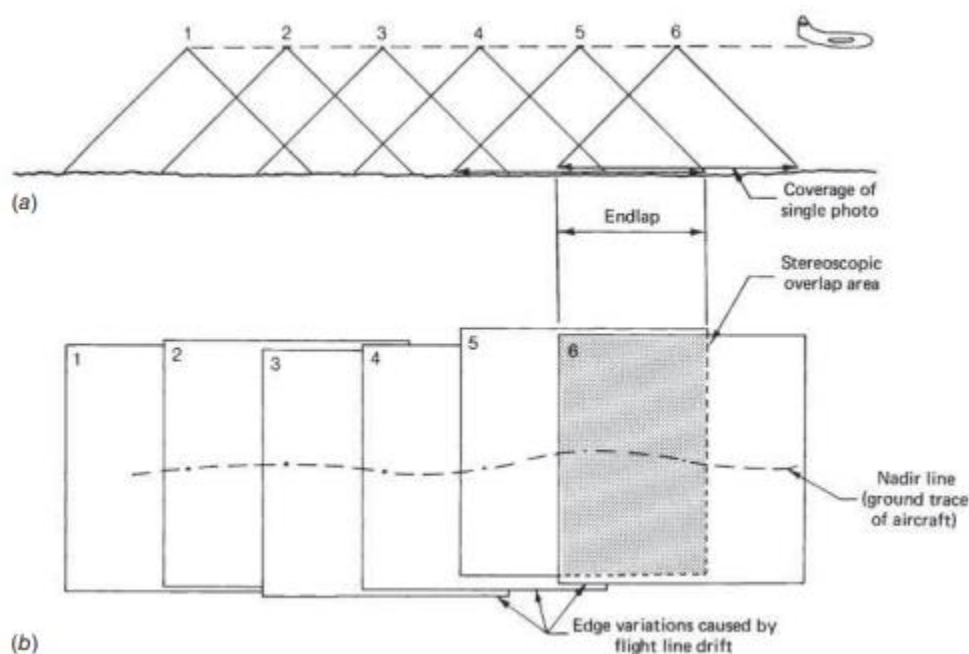


Figure 2.1 Photographic coverage along a flight strip: (a) conditions during exposure; (b) resulting photography.

Successive photographs along a flight strip are taken at intervals that are controlled by the camera intervalometer or software-based sensor control system. The area included in the overlap of successive photographs is called the stereoscopic overlap area. Typically, successive photographs contain 55 to 65% overlap to ensure at least 50% endlap over varying terrain, in spite of unintentional tilt. Figure 2.2

illustrates the ground coverage relationship of successive photographs forming a stereopair having approximately a 60% stereoscopic overlap area.

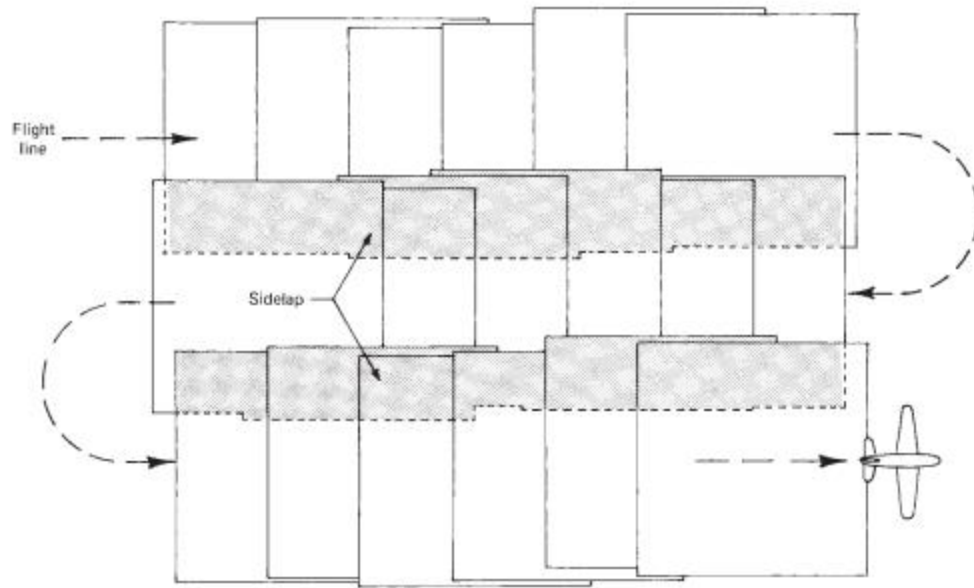
The ground distance between the photo centers at the times of exposure is called the air base. The ratio between the air base and the flying height above ground determines the vertical exaggeration perceived by photo interpreters. The larger the base–height ratio, the greater the vertical exaggeration.



Figure 2.2 **Acquisition of successive photographs yielding a stereopair.**

This greater apparent relief often aids in visual image interpretation. Also, as we will discuss later, many photogrammetric mapping operations depend upon accurate determination of the position at which rays from two or more photographs intersect in space. Rays associated with larger base–height ratios intersect at larger (closer to being perpendicular) angles than do those associated with the smaller (closer to being parallel) angles associated with smaller base–height ratios. Thus larger base–height ratios result in more accurate determination of ray intersection positions than do smaller base–height ratios.

Most project sites are large enough for multiple-flight-line passes to be made over the area to obtain complete stereoscopic coverage. Figure 2.3 illustrates how adjacent strips are photographed. On successive flights over the area, adjacent strips have a sidelap of approximately 30%. Multiple strips comprise what is called a block of photographs.



**Figure 2.3** Adjacent flight lines over a project area.



# المحاضرة السادسة

**Basic Principles of Photogrammetry**

### **Geometric Elements of a Vertical Photograph**

The basic geometric elements of a hardcopy vertical aerial photograph taken with a single-lens frame camera are depicted in Figure 2.4. Light rays from terrain objects are imaged in the plane of the film negative after intersecting at the camera lens exposure station, L. The negative is located behind the lens at a distance equal to the lens focal length,  $f$ . Assuming the size of a paper print positive (or film positive) is equal to that of the negative, positive image positions can be depicted diagrammatically in front of the lens in a plane located at a distance  $f$ . This rendition is appropriate in that most photo positives used for measurement purposes are contact printed, resulting in the geometric relationships shown.

The  $x$  and  $y$  coordinate positions of image points are referenced with respect to axes formed by straight lines joining the opposite fiducial marks recorded on the positive. The  $x$  axis is arbitrarily assigned to the fiducial axis most nearly coincident with the line of flight and is taken as positive in the forward direction of flight. The positive  $y$  axis is located  $90^\circ$  counterclockwise from the positive  $x$  axis. Because of the precision with which the fiducial marks and the lens are placed in a metric camera, the photocoordinate origin,  $o$ , can be assumed to coincide exactly with the principal point, the intersection of the lens optical axis and the film plane. The point where the prolongation of the optical axis of the camera intersects the terrain is referred to as the ground principal point,  $O$ . Images for terrain points A, B, C, D, and E appear geometrically reversed on the negative at  $a$ ,  $b$ ,  $c$ ,  $d$ , and  $e$  and in proper geometric relationship on the positive at  $a$ ,  $b$ ,  $c$ ,  $d$ , and  $e$ .

The  $xy$  photocoordinates of a point are the perpendicular distances from the  $xy$  coordinate axes. Points to the right of the  $y$  axis have positive  $x$  coordinates and points to the left have negative  $x$  coordinates. Similarly, points above the  $x$  axis have positive  $y$  coordinates and those below have negative  $y$  coordinates.

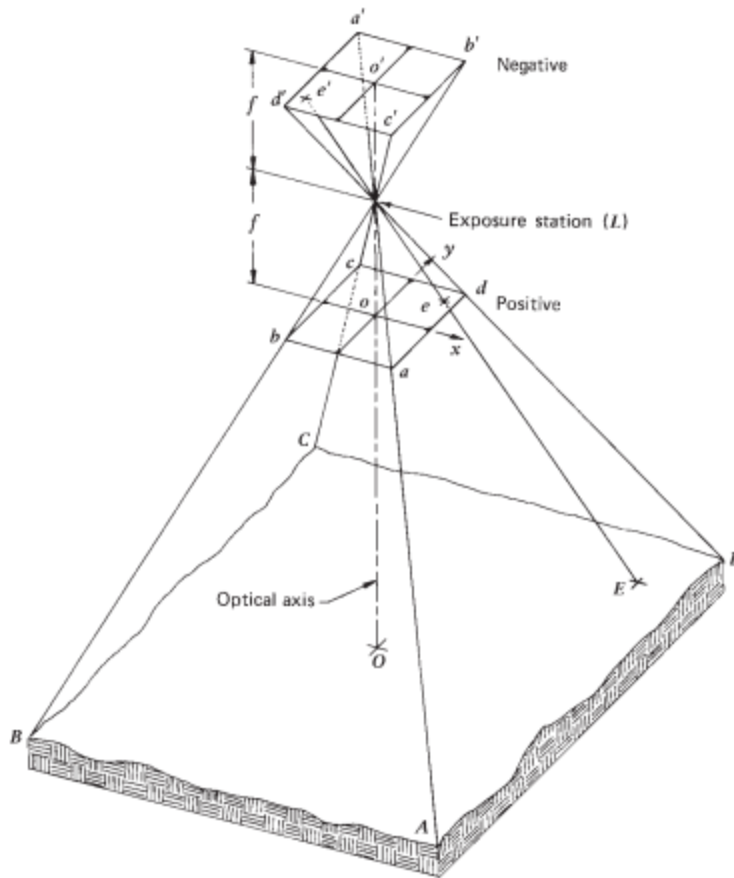


Figure 2.4 Basic geometric elements of a vertical photograph.

### Photocoordinate Measurement

Measurements of photocoordinates may be obtained using any one of many measurement devices. These devices vary in their accuracy, cost, and availability. For rudimentary photogrammetric problems—where low orders of measurement accuracy are acceptable—a triangular engineer’s scale or metric scale may be used. When using these scales, measurement accuracy is generally improved by taking the average of several repeated measurements. Measurements are also generally more accurate when made with the aid of a magnifying lens.

In a softcopy environment, photocoordinates are measured using a raster image display with a cursor to collect “raw” image coordinates in terms of row and column values within the image file. The relationship between the row and column coordinate system and the camera’s fiducial axis coordinate system is determined through the development of a mathematical coordinate transformation between the two systems. This process requires that some points have their coordinates known in both systems. The fiducial marks are used for this purpose in that their positions in the focal plane are determined during the calibration of the camera, and they can be readily measured in the row and column coordinate system.

Irrespective of what approach is used to measure photocoordinates, these measurements contain errors of varying sources and magnitudes. These errors stem from factors such as camera lens distortions, atmospheric refraction, earth curvature, failure of the fiducial axes to intersect at the principal point, and shrinkage or expansion of the photographic material on which measurements are made. Sophisticated photogrammetric analyses include corrections for all these errors. For simple measurements made on paper prints, such corrections are usually not employed because errors introduced by slight tilt in the photography will outweigh the effect of the other distortions.

### 2.3 PHOTOGRAPHIC SCALE

One of the most fundamental and frequently used geometric characteristics of hardcopy aerial photographs is that of photographic scale. A photograph “scale,” like a map scale, is an expression that states that one unit (any unit) of distance on a photograph represents a specific number of units of actual ground distance. Scales may be expressed as unit equivalents, representative fractions, or ratios. For example, if 1 mm on a photograph represents 25 m on the ground, the scale of the photograph can be expressed as 1 mm=25 m (unit equivalents), or 1 /25 000 (representative fraction), or 1:25 000 (ratio). Quite often the terms “large scale” and “small scale” are confused by those not working with expressions of scale on a routine basis. For example, which photograph would have the “larger” scale—a 1:10 000 scale photo covering several city blocks or a 1:50 000 photo that covers an entire city? The intuitive answer is often that the photo covering the larger “area” (the entire city) is the larger scale product. This is not the case. The larger scale product is the 1:10 000 image because it shows ground features at a larger, more detailed, size. The 1:50 000 scale photo of the entire city would render ground features at a much smaller, less detailed size. Hence, in spite of its larger ground coverage, the 1:50 000 photo would be termed the smaller scale product. A convenient way to make scale comparisons is to remember that the same objects are smaller on a “smaller” scale photograph than on a “larger” scale photo. Scale comparisons can also be made by comparing the magnitudes of the representative fractions involved. (That is, 1/ 50 000 is smaller than 1/ 10 000.)

The most straightforward method for determining photo scale is to measure the corresponding photo and ground distances between any two points. This requires that the points be mutually identifiable on both the photo and a map. The scale  $S$  is then computed as the ratio of the photo distance  $d$  to the ground distance  $D$ ,

$$S = \text{photo scale} = \frac{\text{photo distance}}{\text{ground distance}} = \frac{d}{D}$$

#### EXAMPLE 2.1

Assume that two road intersections shown on a photograph can be located on a 1:25 000 scale topographic map. The measured distance between the intersections is 47.2 mm on the map and 94.3 mm on the photograph. (a) What is the scale of the photograph? (b) At that scale, what is the length of a fence line that measures 42.9 mm on the photograph?

**Solution**

(a) The ground distance between the intersections is determined from the map scale as

$$0.0472 \text{ m} \times \frac{25,000}{1} = 1180 \text{ m}$$

By direct ratio, the photo scale is

$$S = \frac{0.0943 \text{ m}}{1180 \text{ m}} = \frac{1}{12,513} \text{ or } 1:12,500$$

(Note that because only three significant, or meaningful, figures were present in the original measurements, only three significant figures are indicated in the final result.)

(b) The ground length of the 42.9-mm fence line is

$$D = \frac{d}{S} = 0.0429 \text{ m} \div \frac{1}{12,500} = 536.25 \text{ m} \text{ or } 536 \text{ m}$$

For a vertical photograph taken over flat terrain, scale is a function of the focal length  $f$  of the camera used to acquire the image and the flying height above the ground,  $H'$ , from which the image was taken. In general,

$$\text{Scale} = \frac{\text{camera focal length}}{\text{flying height above terrain}} = \frac{f}{H'}$$

Figure 2.5 illustrates how we arrive at above Eq. Shown in this figure is the side view of a vertical photograph taken over flat terrain. Exposure station L is at an aircraft

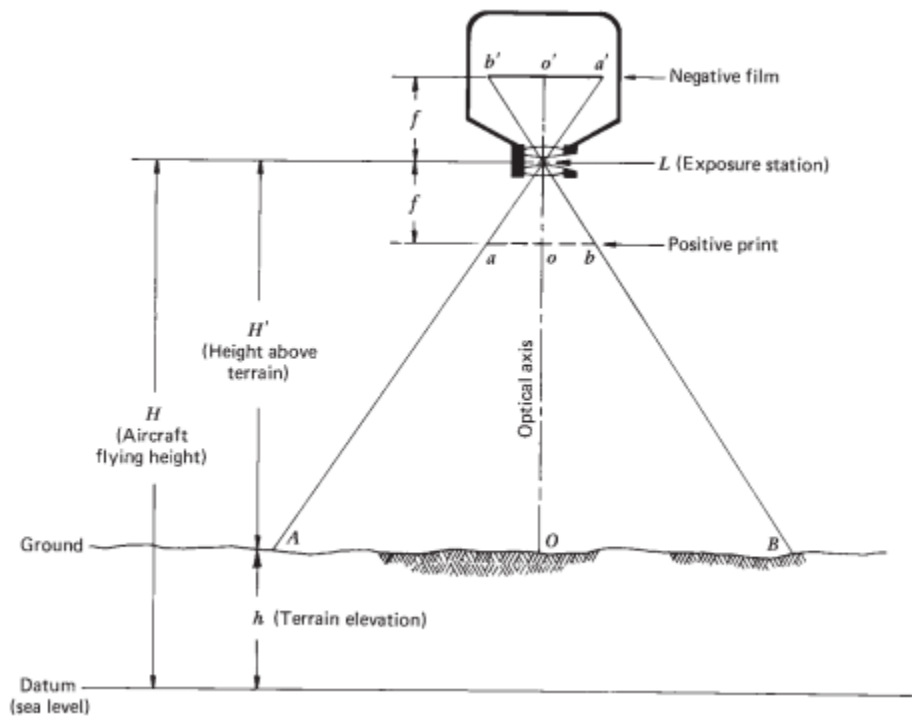


Figure 2.5 Scale of a vertical photograph taken over flat terrain

flying height  $H$  above some datum, or arbitrary base elevation. The datum most frequently used is mean sea level. If flying height  $H$  and the elevation of the terrain  $h$  are known, we can determine  $H'$  by subtraction ( $H' = H - h$ ). If we now consider terrain points  $A$ ,  $O$ , and  $B$ , they are imaged at points  $a'$ ,  $o'$ , and  $b'$  on the negative film and at  $a$ ,  $o$ , and  $b$  on the positive print. We can derive an expression for photo scale by observing similar triangles  $Lao$  and  $LAO$ , and the corresponding photo ( $ao$ ) and ground ( $AO$ ) distances. That is,

$$S = \frac{\overline{ao}}{\overline{AO}} = \frac{f}{H'}$$

or

$$S = \frac{f}{H - h}$$

#### EXAMPLE 2.2

A camera equipped with a 152-mm-focal-length lens is used to take a vertical photograph from a flying height of 2780 m above mean sea level. If the terrain is flat and located at an elevation of 500 m, what is the scale of the photograph?

Solution

$$\text{Scale} = \frac{f}{H-h} = \frac{0.152 \text{ m}}{2780 \text{ m} - 500 \text{ m}} = \frac{1}{15,000} \text{ or } 1:15,000$$

### EXAMPLE 2.3

Assume that a vertical photograph was taken at a flying height of 5000 m above sea level using a camera with a 152-mm-focal-length lens. (a) Determine the photo scale at points A and B, which lie at elevations of 1200 and 1960 m. (b) What ground distance corresponds to a 20.1-mm photo distance measured at each of these elevations?

### Solution

a)

$$S_A = \frac{f}{H-h_A} = \frac{0.152 \text{ m}}{5000 \text{ m} - 1200 \text{ m}} = \frac{1}{25,000} \text{ or } 1:25,000$$

$$S_B = \frac{f}{H-h_B} = \frac{0.152 \text{ m}}{5000 \text{ m} - 1960 \text{ m}} = \frac{1}{20,000} \text{ or } 1:20,000$$

b) The ground distance corresponding to a 20.1-mm photo distance is

$$D_A = \frac{d}{S_A} = 0.0201 \text{ m} \div \frac{1}{25,000} = 502.5 \text{ m or } 502 \text{ m}$$

$$D_B = \frac{d}{S_B} = 0.0201 \text{ m} \div \frac{1}{20,000} = 402 \text{ m}$$

Often it is convenient to compute an average scale for an entire photograph. This scale is calculated using the average terrain elevation for the area imaged. Consequently, it is exact for distances occurring at the average elevation and is approximate at all other elevations. Average scale may be expressed as

$$S_{\text{avg}} = \frac{f}{H-h_{\text{avg}}}$$

where  $h_{\text{avg}}$  is the average elevation of the terrain shown in the photograph.

The result of photo scale variation is geometric distortion. All points on a map are depicted in their true relative horizontal (planimetric) positions, but points on a photo taken over varying terrain are displaced from their true “map positions.” This difference results because a map is a scaled orthographic projection

of the ground surface, whereas a vertical photograph yields a perspective projection. The differing nature of these two forms of projection is illustrated in Figure 2.6. As shown, a map results from projecting vertical rays from ground points to the map sheet (at a particular scale). A photograph results from projecting converging rays through a common point within the camera lens. Because of the nature of this projection, any variations in terrain elevation will result in scale variation and displaced image positions.

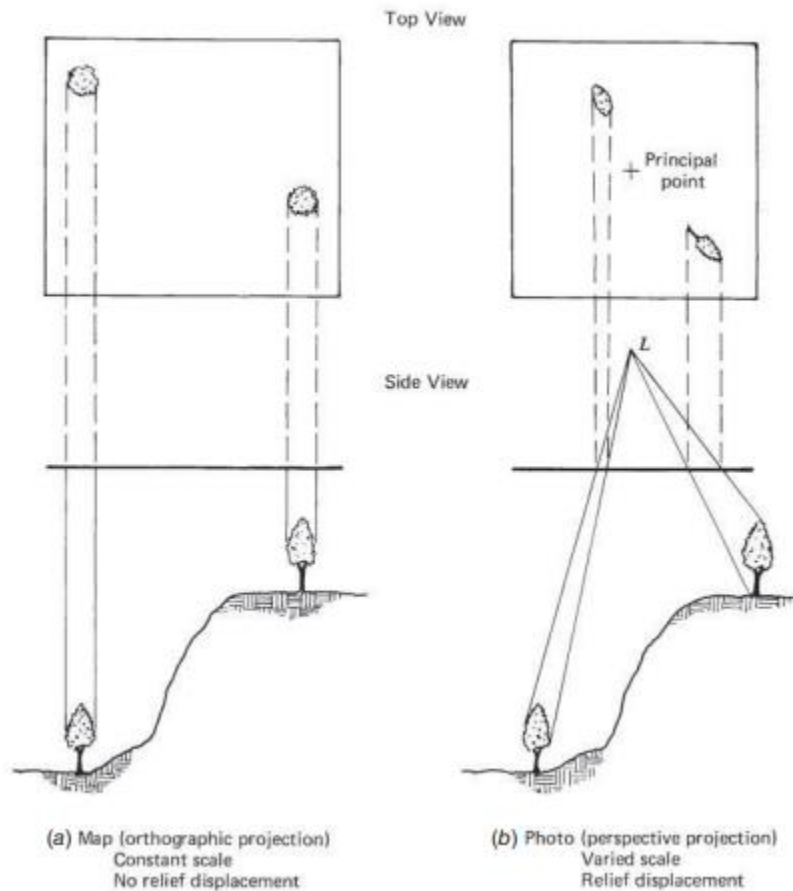


Figure 2.6 Comparative geometry of (a) a map and (b) a vertical aerial photograph. Note differences in size, shape, and location of the two trees.

On a map we see a top view of objects in their true relative horizontal positions. On a photograph, areas of terrain at the higher elevations lie closer to the camera at the time of exposure and therefore appear larger than corresponding areas lying at lower elevations. Furthermore, the tops of objects are always displaced from their bases (Figure 2.6). This distortion is called relief displacement and causes any object standing above the terrain to “lean” away from the principal point of a photograph radially.



# المحاضرة السابعة

**Basic Principles of Photogrammetry**

## AREA MEASUREMENT

The process of measuring areas using aerial photographs can take on many forms. The accuracy of area measurement is a function of not only the measuring device used, but also the degree of image scale variation due to relief in the terrain and tilt in the photography. Although large errors in area determinations can result even with vertical photographs in regions of moderate to high relief, accurate measurements may be made on vertical photos of areas of low relief. Simple scales may be used to measure the area of simply shaped features. For example, the area of a rectangular field can be determined by simply measuring its length and width. Similarly, the area of a circular feature can be computed after measuring its radius or diameter.

### EXAMPLE 2.4

A rectangular agricultural field measures 8.65 cm long and 5.13 cm wide on a vertical photograph having a scale of 1:20,000. Find the area of the field at ground level.

Solution

$$\text{Ground length} = \text{photo length} \times \frac{1}{S} = 0.0865 \text{ m} \times 20,000 = 1730 \text{ m}$$

$$\text{Ground width} = \text{photo width} \times \frac{1}{S} = 0.0513 \text{ m} \times 20,000 = 1026 \text{ m}$$

$$\text{Ground area} = 1730 \text{ m} \times 1026 \text{ m} = 1,774,980 \text{ m}^2 = 177 \text{ ha}$$

The ground area of an irregularly shaped feature is usually determined by measuring the area of the feature on the photograph. The photo area is then converted to a ground area from the following relationship:

$$\text{Ground area} = \text{photo area} \times \frac{1}{S^2}$$

### EXAMPLE 2.5

The area of a lake is 52.2 cm<sup>2</sup> on a 1:7500 vertical photograph. Find the ground area of the lake.

Solution

$$\text{Ground area} = \text{photo area} \times \frac{1}{S^2} = 0.00522 \text{ m}^2 \times 7500^2 = 293,625 \text{ m}^2 = 29.4 \text{ ha}$$

## RELIEF DISPLACEMENT OF VERTICAL FEATURES

### Characteristics of Relief Displacement

In Figure 2.6, we illustrated the effect of relief displacement on a photograph taken over varied terrain. In essence, an increase in the elevation of a feature causes its position on the photograph to be displaced radially outward from the principal point. Hence, when a vertical feature is photographed, relief

displacement causes the top of the feature to lie farther from the photo center than its base. As a result, vertical features appear to lean away from the center of the photograph.

The geometric components of relief displacement are illustrated in Figure 2.7, which shows a vertical photograph imaging a tower. The photograph is taken from flying height  $H$  above datum. When considering the relief displacement of a vertical feature, it is convenient to arbitrarily assume a datum plane placed at the base of the feature. If this is done, the flying height  $H$  must be correctly referenced to this same datum, not mean sea level. Thus, in Figure 2.7 the height of the tower (whose base is at datum) is  $h$ . Note that the top of the tower,  $A$ , is imaged at  $a$  in the photograph whereas the base of the tower,  $A'$ , is imaged at  $a'$ . That is, the image of the top of the tower is radially displaced by the distance  $d$  from that of the bottom. The distance  $d$  is the relief displacement of the tower. The equivalent distance projected to datum is  $D$ . The distance from the photo principal point to the top of the tower is  $r$ . The equivalent distance projected to datum is  $R$ .

We can express  $d$  as a function of the dimensions shown in Figure 2.7. From similar triangles  $AA'A''$  and  $LOA''$ ,

$$\frac{D}{h} = \frac{R}{H}$$

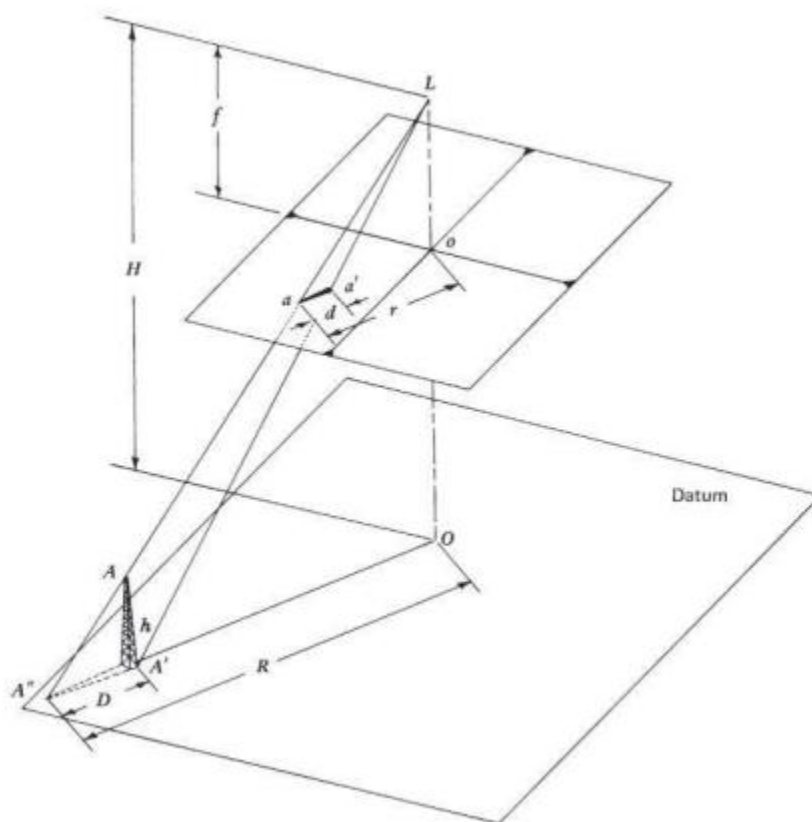


Figure 2.7 Geometric components of relief displacement.

Expressing distances D and R at the scale of the photograph, we obtain

$$\frac{d}{h} = \frac{r}{H}$$

Rearranging the above equation yields

$$d = \frac{rh}{H}$$

where d = relief displacement

r = radial distance on the photograph from the principal point to the displaced image point

h = height above datum of the object point

H = flying height above the same datum chosen to reference h

An analysis of the above equation indicates mathematically the nature of relief displacement seen pictorially. That is, relief displacement of any given point increases as the distance from the principal point increases, and it increases as the elevation of the point increases. Other things being equal, it decreases with an increase in flying height. Hence, under similar conditions high altitude photography of an area manifests less relief displacement than low altitude photography. Also, there is no relief displacement at the principal point (since  $r = 0$ ).

### Object Height Determination from Relief Displacement Measurement

Equation above also indicates that relief displacement increases with the feature height h. This relationship makes it possible to indirectly measure heights of objects appearing on aerial photographs. By rearranging the above equation, we obtain

$$h = \frac{dH}{r}$$

To use this equation, both the top and base of the object to be measured must be clearly identifiable on the photograph and the flying height H must be known. If this is the case, d and r can be measured on the photograph and used to calculate the object height h. (When using the equation above, it is important to remember that H must be referenced to the elevation of the base of the feature, not to mean sea level.)

#### EXAMPLE 2.7

For the photo shown in Figure 3.12, assume that the relief displacement for the tower at A is 2.01 mm, and the radial distance from the center of the photo to the top of the tower is 56.43 mm. If the flying height is 1220 m above the base of the tower, find the height of the tower

Solution

$$h = \frac{dH}{r} = \frac{2.01 \text{ mm} (1220 \text{ m})}{56.43 \text{ mm}} = 43.4 \text{ m}$$

While measuring relief displacement is a very convenient means of calculating heights of objects from aerial photographs, the reader is reminded of the assumptions implicit in the use of the method. We have assumed use of truly vertical photography, accurate knowledge of the flying height, clearly visible objects, precise location of the principal point, and a measurement technique whose accuracy is consistent with the degree of relief displacement involved. If these assumptions are reasonably met, quite reliable height determinations may be made using single prints and relatively unsophisticated measuring equipment.

### Correcting for Relief Displacement

In addition to calculating object heights, quantification of relief displacement can be used to correct the image positions of terrain points appearing in a photograph. Keep in mind that terrain points in areas of varied relief exhibit relief displacements as do vertical objects. If all terrain points were to lie at this common elevation, terrain points A and B would be located at A' and B' and would be imaged at points a' and b' on the photograph. Due to the varied relief, however, the position of point A is shifted radially outward on the photograph (to a), and the position of point B is shifted radially inward (to b). These changes in image position are the relief displacements of points A and B. Figure 2.7 b illustrates the effect they have on the geometry of the photo. Because A' and B' lie at the same terrain elevation, the image line a' b' accurately represents the scaled horizontal length and directional orientation of the ground line AB.

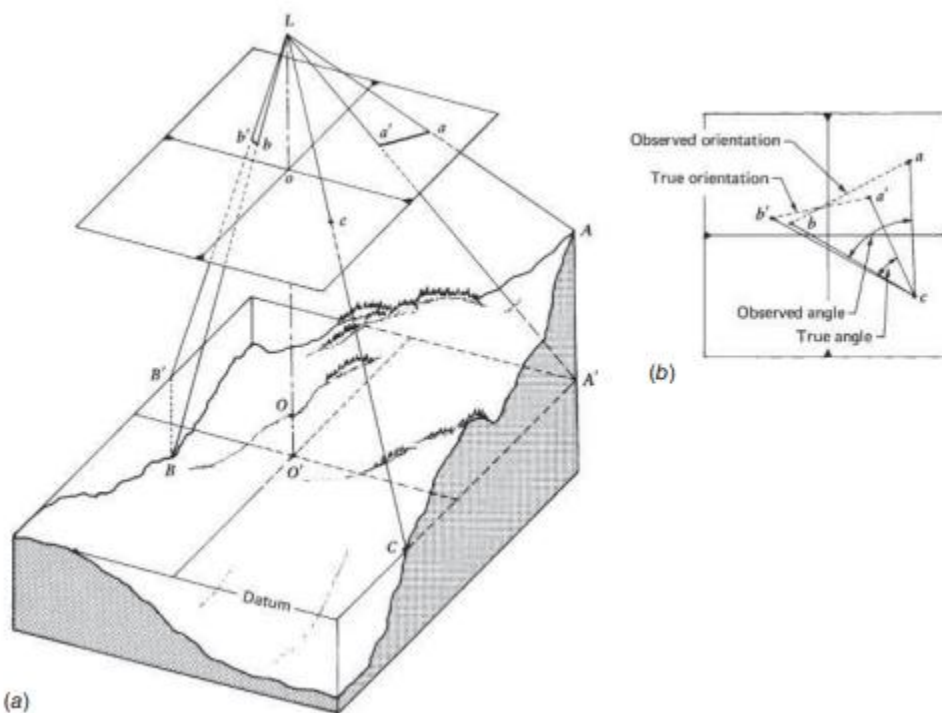


Figure 2.7 Relief displacement on a photograph taken over varied terrain: (a) displacement of terrain points; (b) distortion of horizontal angles measured on photograph.

When the relief displacements are introduced, the resulting line  $ab$  has a considerably altered length and orientation. Angles are also distorted by relief displacements. In Figure 2.7b, the horizontal ground angle  $ACB$  is accurately expressed by  $a'cb'$  on the photo. Due to the displacements, the distorted angle  $acb$  will appear on the photograph. Note that, because of the radial nature of relief displacements, angles about the origin of the photo (such as  $aob$ ) will not be distorted.

Relief displacement can be corrected for by above Eq. to compute its magnitude on a point-by-point basis and then laying off the computed displacement distances radially (in reverse) on the photograph. This procedure establishes the datum-level image positions of the points and removes the relief distortions, resulting in planimetrically correct image positions at datum scale. This scale can be determined from the flying height above datum ( $S=f/H$ ). Ground lengths, directions, angles, and areas may then be directly determined from these corrected image positions.

#### EXAMPLE 2.8

Referring to the vertical photograph depicted in Figure 2.7, assume that the radial distance  $r_a$  to point A is 63.84 mm and the radial distance  $r_b$  to point B is 62.65 mm. Flying height  $H$  is 1220 m above datum, point A is 152 m above datum, and point B is 168 m below datum. Find the radial distance and direction one must lay off from points  $a$  and  $b$  to plot  $a_0$  and  $b_0$

Solution

$$d_a = \frac{r_a h_a}{H} = \frac{63.84 \text{ mm} \times 152 \text{ m}}{1220 \text{ m}} = 7.95 \text{ mm} \quad (\text{plot inward})$$

$$d_b = \frac{r_b h_b}{H} = \frac{62.65 \text{ mm} \times (-168 \text{ m})}{1220 \text{ m}} = -8.63 \text{ mm} \quad (\text{plot outward})$$

# المحاضرة الثامنة

**Natural Land Resources Observation Systems**

## CHAPTER THREE

### Natural Land Resources Observation Systems

#### Landsat Series

The US space agency launched the first satellite of Landsat series (1-7) in 1972 and was used in monitoring the Earth and environmental changes and then the rest of the satellites of the series were launched. These sensors were of three types:

- Return beam vidicon
- MultiSpectral Scanner
- Thematic mapper

#### Characteristics of Landsat satellites 1-3

The Landsat series passes in orbits 9 degrees away from the poles. , they orbit the Earth every 103 minutes, about 14 cycles a day. The satellites intersect the equator at an angle of 9 degrees. To provide nearly complete coverage of the Earth's surface, these satellites take images at length equal 185-km

The first generation of Landsat satellites (1-3) contains two types of sensors:

1. RBV (3-bands)
2. Multi - Spectral Scanner (MSS) with four spectral bands

The following table shows the general specifications of the Landsat satellite series



**Table 1.** Landsat mission dates.

Satellite	Launch	Decommissioned	Sensors
Landsat 1	July 23, 1972	January 6, 1978	MSS/RBV
Landsat 2	January 22, 1975	July 27, 1983	MSS/RBV
Landsat 3	March 5, 1978	September 7, 1983	MSS/RBV
Landsat 4	July 16, 1982	June 15, 2001	MSS/TM
Landsat 5	March 1, 1984	2013	MSS/TM
Landsat 6	October 5, 1993	Did not achieve orbit	ETM
Landsat 7	April 15, 1999	Operational	ETM+
Landsat 8	February 11, 2013	Operational	OLI/TIRS

**Table 2.** MSS band designations.

Landsats 1,2,3 spectral bands	Landsats 4,5 spectral bands	Wavelength (micrometers)	Resolution (meters)	Use
Band 4–green	Band 1–green	0.5–0.6	80	Emphasizes sediment-laden water and delineates areas of shallow water.
Band 5–red	Band 2–red	0.6–0.7	80	Emphasizes cultural features.
Band 6–near IR	Band 3–near IR	0.7–0.8	80	Emphasizes vegetation boundary between land and water, and landforms.
Band 7–near IR	Band 4–near IR	0.8–1.1	80	Penetrates atmosphere haze best; emphasizes vegetation, boundary between land and water, and landforms.

Instrument-specific relative spectral response functions may be viewed and compared using the Spectral Viewer tool: [http://landsat.usgs.gov/tools\\_spectralViewer.php](http://landsat.usgs.gov/tools_spectralViewer.php).

### Landsat Characteristics (4, 5)

Landsat (4, 5) was launched in orbits near the pole in conjunction with the sun and was lowered to improve the spatial resolution of the sensors, each satellite crossing the equator at 9:45 am and taking 99 minutes (14.5) cycles per day, as shown in Table (1).

There are two types of Landsat sensors (4 and 5),

- Multi-Spectral Scanner (MSS), and
- Thematic Mapper (TM).
- 

The Landsat (MSS, TM) sensor system (4, 5) captures the reflected and emitted radiation from the Earth's surface in Visible and Near Infrared (NIR) .

### Landsat satellites (6 and 7)

The space shuttle, which carried Landsat 6 was fail , was unable to reach orbit. After the successful launch of the Landsat 7 satellite, the improvements that added to Landsat 6 were transferred to Landsat 7.

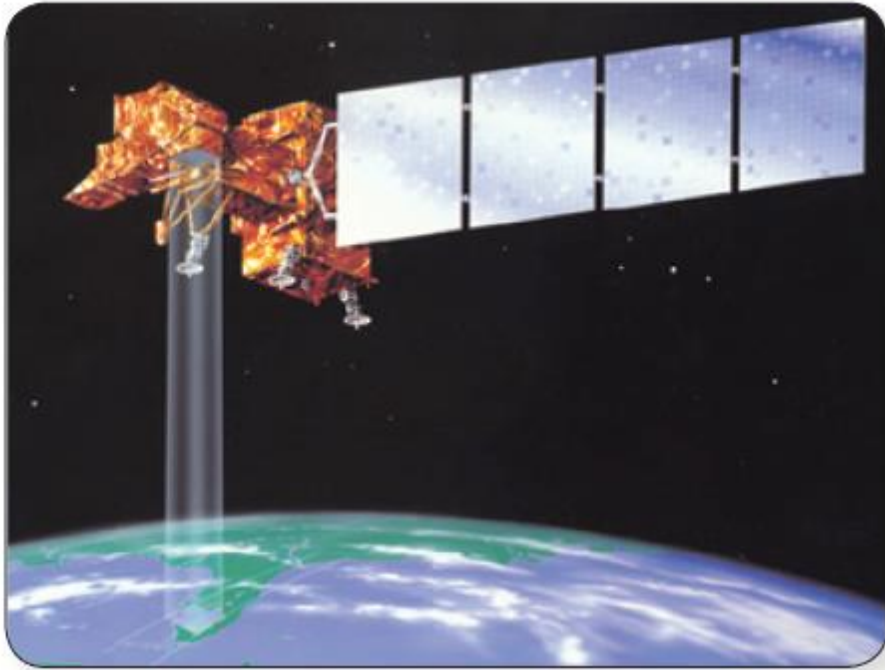
The Landsat 7 has an enhanced Enhanced Thematic Mapper (ETM +), which is similar to the TM sensor, but is more sophisticated, adding a new pancrometric band with a spatial accuracy of 15 and an infrared thermal band. It also has a higher radiometric accuracy and resolution Accuracy than the sensor (MSS)

The following table shows the spectral domains of TM in Landsat (4, 5) and ETM + In Landsat 7 which operates in seven waves, with the characteristics of each field.

**Table 3. TM and ETM+ band designations.**

Spectral bands	Wavelength (micrometers)	Resolution (meters)	Use
Band 1–blue-green	0.45–0.52	30	Bathymetric mapping; distinguishes soil from vegetation; deciduous from coniferous vegetation.
Band 2–green	0.52–0.61	30	Emphasizes peak vegetation, which is useful for assessing plant vigor.
Band 3–red	0.63–0.69	30	Emphasizes vegetation slopes.
Band 4–reflected IR	0.76–0.90	30	Emphasizes biomass content and shorelines.
Band 5–reflected IR	1.55–1.75	30	Discriminates moisture content of soil and vegetation; penetrates thin clouds.
Band 6–thermal	10.40–12.50	120	Useful for thermal mapping and estimated soil moisture.
Band 7–reflected IR	2.08–2.35	30	Useful for mapping hydrothermally altered rocks associated with mineral deposits.
Band 8–panchromatic (Landsat 7)	0.52–0.90	15	Useful in ‘sharpening’ multispectral images.

Instrument-specific relative spectral response functions may be viewed and compared using the Spectral Viewer tool: [http://landsat.usgs.gov/tools\\_spectralViewer.php](http://landsat.usgs.gov/tools_spectralViewer.php).



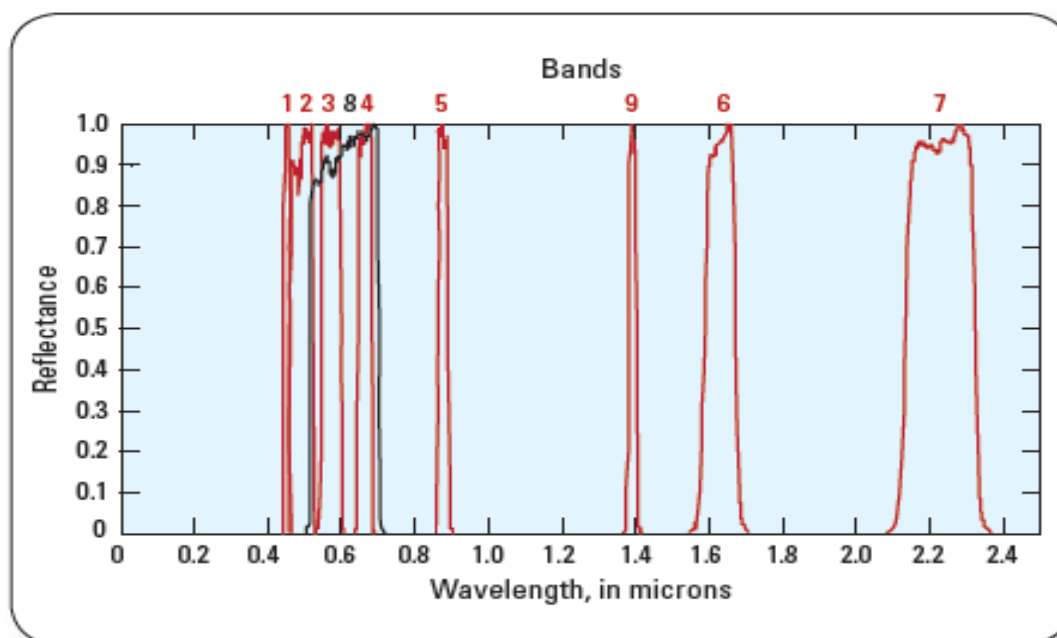
**Figure 2.** Landsat 7 satellite.

**Landsat 8 LC08**

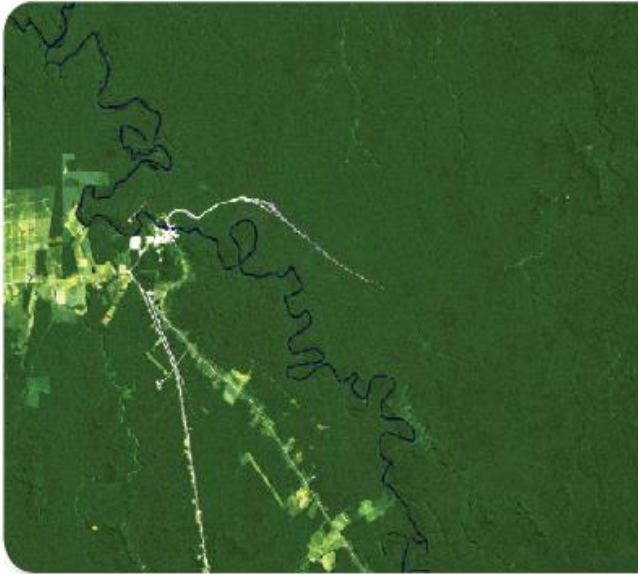
**Table 4.** OLI and TIRS band designations.

Spectral bands	Wavelength (micrometers)	Resolution (meters)	Use
Band 1—coastal/aerosol	0.43–0.45	30	Increased coastal zone observations.
Band 2—blue	0.45–0.51	30	Bathymetric mapping; distinguishes soil from vegetation; deciduous from coniferous vegetation.
Band 3—green	0.53–0.59	30	Emphasizes peak vegetation, which is useful for assessing plant vigor.
Band 4—red	0.64–0.67	30	Emphasizes vegetation slopes.
Band 5—near IR	0.85–0.88	30	Emphasizes vegetation boundary between land and water, and landforms.
Band 6—SWIR 1	1.57–1.65	30	Used in detecting plant drought stress and delineating burnt areas and fire-affected vegetation, and is also sensitive to the thermal radiation emitted by intense fires; can be used to detect active fires, especially during nighttime when the background interference from SWIR in reflected sunlight is absent.
Band 7—SWIR-1	2.11–2.29	30	Used in detecting drought stress, burnt and fire-affected areas, and can be used to detect active fires, especially at nighttime.
Band 8—panchromatic	0.50–0.68	15	Useful in 'sharpening' multispectral images.
Band 9—cirrus	1.36–1.38	30	Useful in detecting cirrus clouds.
Band 10—TIRS 1	10.60–11.19	100	Useful for mapping thermal differences in water currents, monitoring fires and other night studies, and estimating soil moisture.
Band 11—TIRS 2	11.50–12.51	100	Same as band 10.

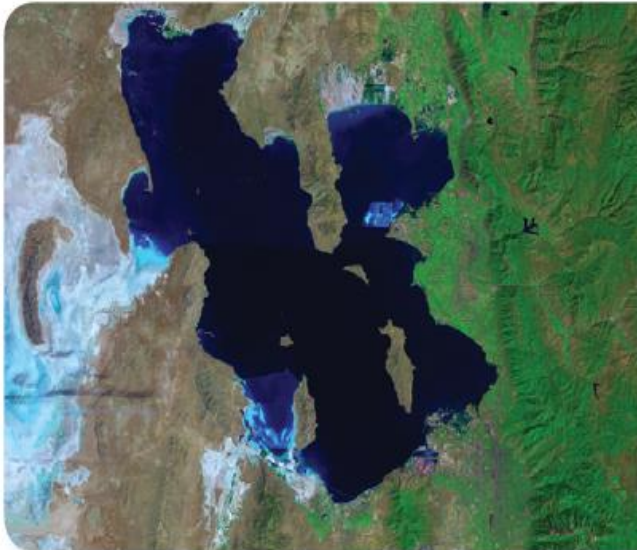
Instrument-specific relative spectral response functions may be viewed and compared using the Spectral Viewer tool: [http://landsat.usgs.gov/tools\\_spectralViewer.php](http://landsat.usgs.gov/tools_spectralViewer.php).



**Figure 3.** Landsat 8 Operational Land Imager (OLI) relative spectral response functions.



Dam construction and progression of deforestation in Rondônia, Brazil. The image on the left was acquired on June 24, 1984; the right image on August 6, 2011.



The Great Salt Lake in Utah. Each image was created by mosaicking four Landsat scenes. The left image represents the area in August 1985; the right image in September 2010.

### SPOT Satellites Series

The first satellite of the Spot series was launched from the Courmoulin launch range in French Guiana in 1986, carrying the first Ground survey sensor, containing a linear matrix sensor. Spot features other programs with a light-emitting device, a linear array sensor and a holographic capability. After the launch of the first satellite of the Spot series in 1986, Spot (2) was launched in 1990, followed by Spot 3 in 1993, which stopped in 1996, while Spot (1 and 2) still working in their orbits.

### **Sensors on board SPOT 1 – 3**

Spot has two high resolution visual (HRV) and magnetic tape recorders. The camera employs two types of sensor systems:

#### **1. Pancromatic mode (P)**

A wide spectral band, with the exception of blue, is sensed with a spatial resolution of up to 10 m. It is mainly intended for studies that require geometrical detail.

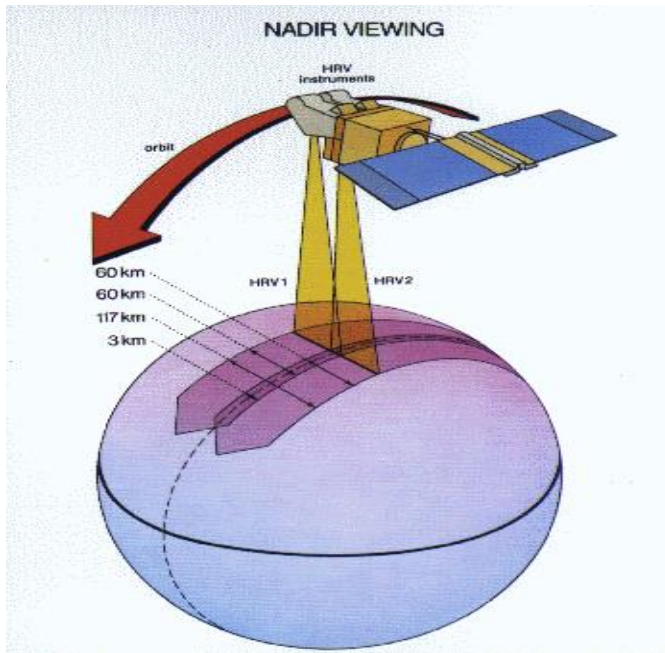
#### **2. Multispectral mode (XS)**

Three spectral bands are sensed:

- XS1 (0.50 – 0.59)  $\mu\text{m}$  (Green band)
- XS2(0.61-0.68)  $\mu\text{m}$  (Red Band)
- XS3(0.79 – 0.89)  $\mu\text{m}$  (NIR band)

By gaining the data recorded in this set of spectral beams, composite color images can be produced with a precision resolution of 20 m.

The figure below shows the HRV sensor in Spot Satellite



# المحاضرة التاسعة

**Global Positioning System (GPS)**



## **CHAPTER FOUR**

### **Global Positioning System (GPS)**

The GPS or “Global Positioning System” is a system for calculating position from signals sent by a network of satellites. The satellites orbit the earth in a geosynchronous orbit, at an altitude of 20.2 km, forming a constellation of satellites, so that at least 4 of them are visible from any point on the planet.

The designation of the initials (G) means GPS, and location is a geographical indication of a place relative to what surrounds it. The location of any object was previously calculated by calculating the distance between the body and the nearest object, taking into account the direction or angle.

### **Global Positioning System (GPS) Global positioning system**

GPS is a global positioning system, the location is a geographical indication of a place relative to its surroundings. The location of any object was previously calculated by calculating the distance between the object and the nearest object, taking into account the direction or angle.

When coordinate systems appeared such as :

- Geographic coordinate system (latitude and longitude)
- Universal Network Transverse Mercator - UTM

It is possible to determine the second coordinate of any object and in a high degree of accuracy, but there are some disadvantages, including:

1. Identify the small objects is not accurate in some applications.
2. The difficulty of locating the objects from maps or aerial and space images in areas characterized by low diversity in the earth features such as deserts, dense forests and water bodies.
3. The aforementioned coordinate systems do not fit in the positioning of moving targets.

At present time, due to availability of satellites, it has become possible to locate and track moving targets, by determining the third coordinate of any target or point on the earth surface, whether the target is fixed or moving.

GPS is defined as a satellite-based navigation system to provide the location to user with speed and time data whether on land, at sea, in the atmosphere, under any weather conditions, by using radio waves.

## **The Principal of the GPS**

The work of the system depends on the knowledge of the distance between two points at a specific time and known. The first point represents the location of a device transmitting a signal at a very precise and precise time, the second point representing the location of a device receiving that signal and the time taken by the signal in access to the receiver is calculated from the following equation:

$$\textit{Distance between the transmitter and receiver} = \textit{time} * \textit{signal velocity}$$

The exact distance between the device that the signal and the device received is determined. From the location of the transmitter, the position of the receiver is determined by a set of mathematical equations.

In the Global Positioning System (GPS):

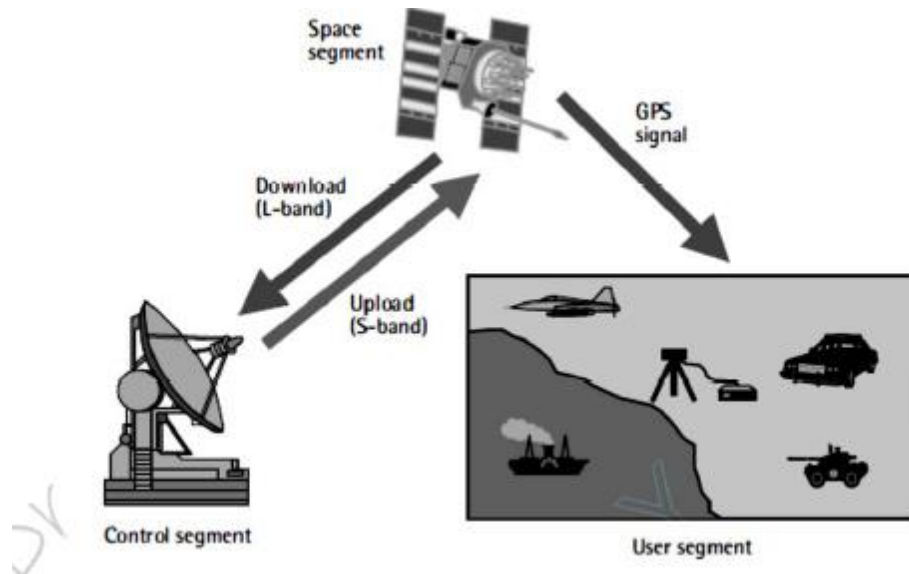
- The device that sent the signal is a group of satellites that are termed it by the *space segment* specialized and distributed in orbits around the earth.
- The signals that are sent by these satellites are the *Radio Waves*.
- The *Receiving device* is called *User Segment*,
- The *Control Segment* for Control and correct information,
- It is worth noting that the receiver does not identify the location only, but is able to calculate the height and time and speed.
- To find the location and altitude throughout GPS, must be at least four satellites in the space that *Receiving* signal from the User unit in same time.

## **Advantages of GPS**

1. Provides user three-dimensional information "astronomical location and altitude above sea level" in addition to the time and speed accurately , continuously during the all hours of the day hours and for fixed and moving targets.
2. The system can be used under any weather conditions and even in areas where the sky is partially obscured by clouds or plants, but it can not be used when the sky is completely obscured , as inside the house or under bridges.
3. GPSs Covers most of the world and is used in areas of military operations.
4. It is flexible in providing the information for user according desired axes system.
5. Low cost and great benefit.
6. Available for civil use other than the Russian system "GLONASS", which is reserved only for military use.

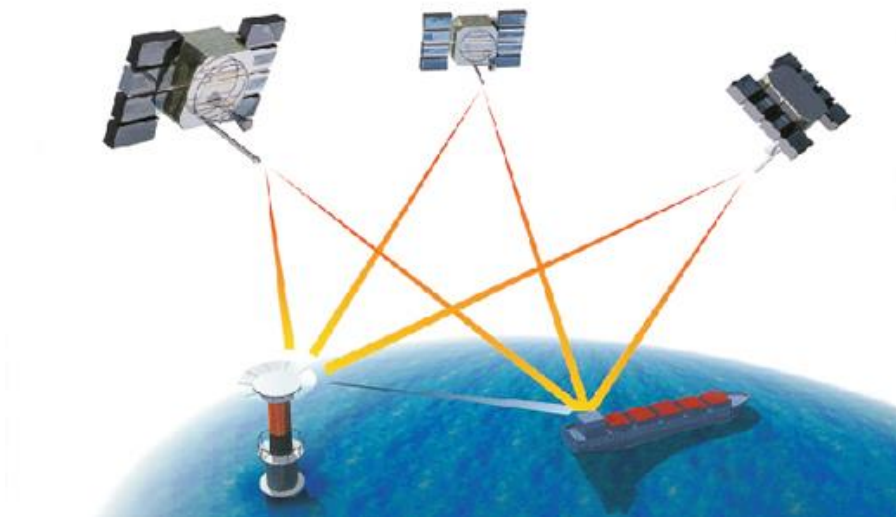
## **GPS Components**

This system consists of three basic units and three sub-units that connect the main units and as shown below:



### 1. *Space Unit:*

The *Space unit* consists of twenty-seven satellites, twenty-four of them in the working position and three satellites use it when needed (in case of failure of one of the satellites). Orbiting on the earth in six precisely defined orbits with four satellites in each orbit and at an approximate height of "2,000 km" completing its orbit around the earth every 12 hours. The orbits of the satellites are 55 degrees below the equator that.



These satellites send the radio waves, specifically L waves , with a wavelength of 19,40 - 76.9 cm. Two signals, L1 at 1575.42 Mhz and L2 at a frequency of 1227.6 Mhz, are generated and controlled by four atomic clocks mounted on these satellites.

There are unintended errors by receiver performance or to the engineering relationship between the satellites, we can reduce these errors and treatment . The decline in GPS performance led to the development a new type of GPS called the Differential Global Positioning System (DGPS). The system works with two or more receptors, one of them is fixed at the point that knowing its location precisely and its represent as a reference for the secondary receiver, (Dynamic receiver).



DGPS offers a probability of accuracy ranging from 1 - 10 m for moving targets and is limited to a few centimeters and can be a few mm for fixed targets.

## *2. Control Segment*

GPS satellites are affected by a number of factors, including:

- a. The gravity of the sun
  - b. moon Gravity
  - c. Solar wind
  - d. The electronic units in the satellite itself
- Thus, through the control unit, it will be control the paths of GPS satellites and correct it information and monitor the devices work carried by the satellites.

- There is a major control unit located in Colorado and five GPS observation stations, two of them in the Pacific Ocean, one in the Indian Ocean, one in the Atlantic Ocean and the fifth located near the main control unit.
- The stations are connected to three main antennas, one in the Pacific Ocean, the other in the Indian Ocean and the third in the Atlantic Ocean.
- The monitoring stations receive data from the satellites every day and send them to the main control station to process them and return them to observation stations that sent by antennas to the satellites.

### 3. *User Segment*

There are several types of user units, all kinds consist of five main parts:

- 1) An antenna operating in the L-wave range of 19.40 - 76.90 cm to capture the transmitted signals from satellites.
- 2) Receiver for tracking signals and performs the measurements.
- 3) Data processor to apply mathematical equations to calculate the location and so on.
- 4) Storage unit for data processing or retrieve the data processing.
- 5) Input unit and display unit.



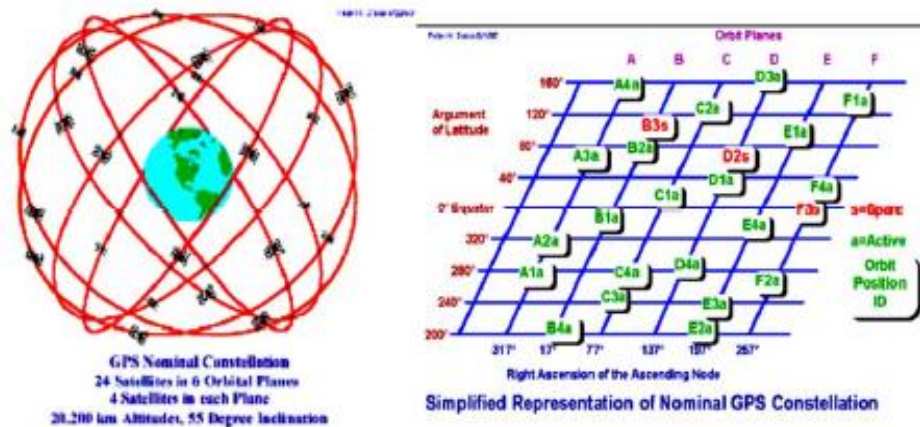
The receiver antenna collects the satellites signals and converts it from electromagnetic waves into electronic currents that are sensitive to the receiver of radio frequencies.

The channels inside receiver will perform distinguish, separate, sort and classify these currents. After the identification these frequency, the processor applies a number of mathematical equations to the data that was classified at a previous stage in order to calculate the location, then, the results will sent to the display unit or stored until needed.

The most important advantages that the user is looking for receivers are:

- 1) High degree of accuracy in measurements work.
- 2) High ability to track signals
- 3) The ability to immediate correction in the field
- 4) Light weight and cheap price.
- 5) High resistance to frost and heat
- 6) Multiple receive channels
- 7) The possibility of making digital maps immediately
- 8) Possibility to use different languages.





## Uses of Global Positioning System GPS in Agriculture:

- 1) Planning, mapping and surveying agricultural land.
- 2) Identify the location of agricultural lands, nature reserves, forests, wells and facilitating access to these areas.
- 3) Calculate the area of fields and agricultural lands
- 4) Assist in the interpretation of aerial and satellites images for agricultural purposes as a method of matching the agricultural region on the earth and its location in satellites images.
- 5) Helps in the correction stage of satellites images .

## Uses of GPS in Transportation:

- 1) Direct the various of transport "Maritime transport, road transport, air transport " and identify it location and pathways and directions of the process and tracking and easier ways to reach the required places.
- 2) Assistance in the launch of spacecraft and the identification of orbits and assistance in taking off and landing.
- 3) Help in improve the performance of landing and takeoffs especially in bad weather conditions.

### **Uses of GPS in Geology:**

- 1) Assisting in prospecting by locating the drilling rigorously at sea or at sea and following up and directing the movement of the exploration vehicles and supply convoys in the desert areas.
- 2) Helps to identify potential earthquake areas and severity of these tremors

### **Uses of GPS in other applications:**

- 1) to be used by wireless operators in synchronizing the stations of the terrestrial digital network and satellites (artificial satellites)
- 2) Rescue and search operations to rescue those injured in crashes, accidents, ship drowning, tracing and forest fires
- 3) Monitoring the movement of migratory and wild birds and wild and marine animals
- 4) A main source for supplying GIS with data.

# المحاضرة العاشرة

**Principle of Geographic Information System**

## CHAPTER FIVE

### Principles of GIS

#### Scope of Geographic Information System

The appearance of geographic information systems (GIS) in the mid-1960s reflects the progress in computer technology and the influence of quantitative revolution in geography. GIS has evolved dramatically from a tool of automated mapping and data management in the early days into a capable spatial data-handling and analysis technology and, more recently, into geographic information science (GISc).

The commercial success since the early 1980s has gained GIS an increasingly wider application. Therefore, to give GIS a generally accepted definition is difficult nowadays. An early definition by Calkins and Tomlinson (1977) states:

" A geographic information system is an integrated software package specifically designed for use with geographic data that performs a comprehensive range of data handling tasks. These tasks include data input, storage, retrieval and output, in addition to a wide variety of descriptive and analytical processes. "

From the definition, it becomes clear that GIS handles geographic data, which include both spatial and attribute data that describe geographic features. Second, the basic functions of GIS include data input, storage, processing, and output. The basic concept of GIS is one of location and spatial distribution and relationship (Fedra, 1996). The backbone analytical function of GIS is overlay of spatially referenced data layers, which allows delineating their spatial relationships. However, it is also true that data used in GIS are predominantly static in nature, and most of them are collected on a single occasion and then archived.

GIS today is far broader and harder to define. Many people prefer to define its domain as geographic information science and technology (GIS&T), and it has become imbedded in many academic and practical fields. The GIS&T field is a loose coalescence of groups of users, managers, academics, and professionals all working with geospatial information. Each group has a distinct educational and

“cultural” background. Each identifies itself with particular ways of approaching particular sets of problems.

Over the course of development, many disciplines have contributed to GIS. Therefore, GIS has many close and far “relatives.” Disciplines that traditionally have researched geographic information technologies include cartography, remote sensing, geodesy, surveying, photogrammetry, etc. Disciplines that traditionally have researched digital technology and information include computer science in general and databases, computational geometry, image processing, pattern recognition, and information science in particular. Disciplines that traditionally have studied the nature of human understanding and its interactions with machines include particularly cognitive psychology, environmental psychology, cognitive science, and artificial intelligence.

In developing a core curriculum for GIS, the University Consortium for Geographic Information Science (UCGIS, 2003) suggests that “GIS&T should not be defined by merely linking segments of the traditional domains (e.g., cartography, remote sensing, statistical analysis, locational analysis, etc.), but rather by placing the emphasis directly upon concepts and methods for geographic problem solving in a computational environment.” GIS should not be viewed merely as a collection of tools and techniques. Rather, the scope of GIS&T represents “a body of knowledge that focuses in an analytic fashion upon various aspects of spatial and spatiotemporal information and therefore constitutes, in some of its aspects, a science” (UCGIS, 2003).

GIS has been called or defined as an enabling technology because of the breadth of uses in the following disciplines as a tool. Disciplines that traditionally have studied the earth, particularly its surface and near surface in either physical or human aspect, include geology, geophysics, oceanography, agriculture, ecology, biogeography, environmental science, geography, global science, sociology, political science, epidemiology, anthropology, demography, and many more.

When the focus is largely on the utilization of GIS&T to attain solutions to real-world problems, GIS has more of an engineering flavor, with attention being given to both the creation and the use of complex tools and techniques that embody the concepts of GIS&T.

Among the management and decision-making groups, for instance, GIS finds its intensive and extensive applications in resource inventory and management, urban planning, land records for taxation and ownership control, facilities management, marketing and retail planning, vehicle routing and scheduling, etc. Each application area of GIS requires a special treatment and must examine data sources, data models, analytical methods, problem-solving approaches, and planning and management issues.

## **Raster GIS and Capabilities**

In GIS, data models provide rules to convert real geographic variation into discrete objects. There are generally two major types of data models: raster and vector. Figure 1.3 illustrates these two GIS data models. A raster model divides the entire study area into a regular grid of cells in specific sequence (similar to pixels in digital remote sensing imagery), with each cell containing a single value.

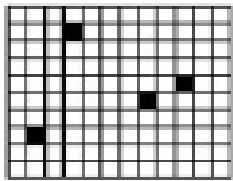

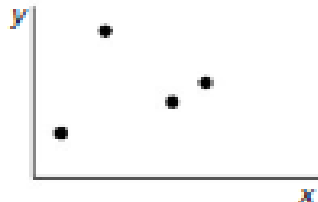
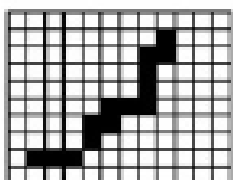

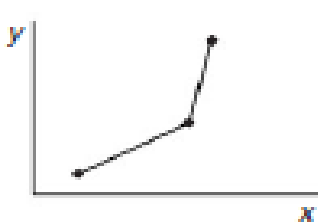
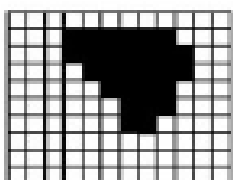

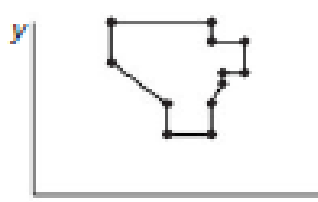
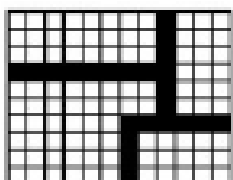
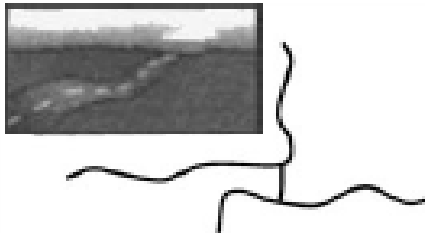
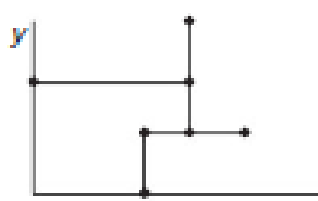
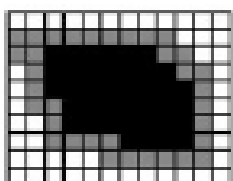
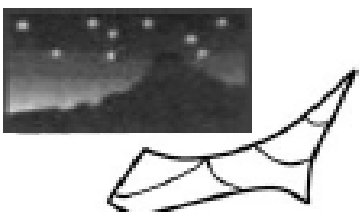
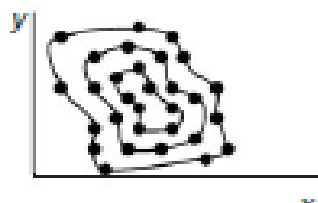
The raster model is a space-filling model because every location in the study area corresponds to a cell in the raster. A set of data describing a single characteristic for each location (cell) within a bounded geographic area forms a raster data layer. Within a raster layer, there may be numerous zones (also named patches, regions, and polygons), with each zone being a set of contiguous locations that exhibit the same value. All individual zones that have the same characteristics form a class of a raster layer. Each cell is identified by an ordered pair of coordinates (row and column numbers) and does not have an explicit topological relationship with its neighboring cells.

Important raster datasets used in GIS include digital land use and land cover data, DEMs of various resolutions, digital orthoimages, and digital raster graphics (DRGs) produced by the U.S. Geological Survey. Because remote sensing generates digital images in raster format, it is easier to interface with a raster GIS than any other type. It is believed that remote sensing images and information extracted from such images, along with GPS data, have become major data sources for raster GIS (Lillesand et al., 2008).

The analytical capabilities of a raster GIS result directly from the application of traditional statistics and algebra to process spatial data—raster data layers. Raster processing operations are commonly grouped into four classes based on the set of cells in the input layer(s) participating in the computation of a value for a cell in the output layer (Gao et al., 1996). They are (1) per-cell or local operation, (2)

perneighborhood or focal operation, (3) per-zone or zonal operation, and (4) per-layer or global operation. During a per-cell operation, the value of each new pixel is defined by the values of the same pixel on the input layer(s), and neighboring or distant pixels have no effect.

In a per-neighborhood operation, the value of a pixel on the new layer is determined by the local neighborhood of the pixel on the old data layer. Per-zone operations treat each zone as an entity and apply algebra to the zones. Per-layer or global operations apply algebra to all cells in the old layer to the value of a pixel on the new layer. A suite of raster processing operations may be logically organized in order to implement a particular data-analysis application. Cartographic modeling is such a technique, which builds models within a raster GIS by using map algebra (Tomlin, 1991).

The raster view of the world	Happy valley spatial entities	The vector view of the world
	 <p data-bbox="695 520 873 552">Points: hotels</p>	
	 <p data-bbox="695 814 873 846">Lines: ski lifts</p>	
	 <p data-bbox="695 1094 873 1125">Areas: forest</p>	
	 <p data-bbox="683 1381 878 1413">Network: roads</p>	
	 <p data-bbox="667 1644 902 1675">Surface: elevation</p>	

**FIGURE 1.3** Raster and vector data models. (Adapted from Heywood et al. 1998; used with permission from Prentice Hall.)



The method of map algebra, first introduced by Tomlin, involves the application of a sequence of processing commands to a set of input map layers to generate a desired output layer. Each processing operation is applied to all the cells in the layers, and the result is saved in a new layer. All the layers are referenced to a uniform geometry, usually that of a regular square grid. Map algebra is quite similar to traditional algebra. Most of the traditional mathematical capabilities plus an extensive set of advanced map-processing functions are used (Berry, 1993).

Many raster GIS of the current generation have made a rich set of functions available to the user for cartographic modeling. Among these functions are overlay, distance and connectivity mapping, neighborhood analysis, topographic shading analysis, watershed analysis, surface interpolation, regression analysis, clustering, classification, and visibility analysis (Berry, 1993; Gao et al., 1996). The overlay functions, for example, may be categorized into two approaches: location-specific overlay and category-specific overlay. The first approach involves the vertical spearing of a set of layers; that is, the values assigned are a function of the point-by-point coincidence of the existing layers.

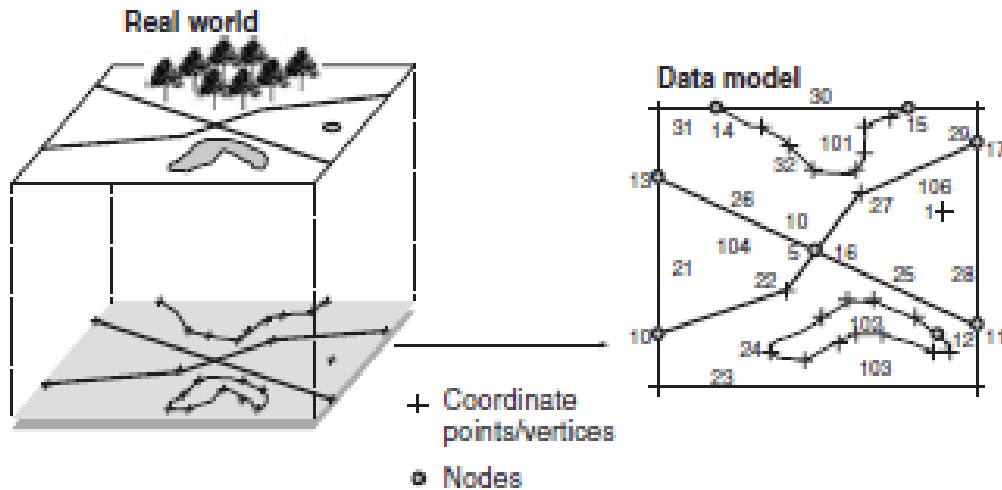
Environmental modeling typically involves the manipulation of quantitative data using basic arithmetic operations, as well as simple descriptive statistical parameters. The type of function used for a overlaying may vary in the light of the nature of the data (e.g., nominal, ratio, etc.) being processed and use of the resulting data.

An extreme case of this approach is dealing with Boolean images that only have values 1 and 0. Simple arithmetic operations in this case are used to perform logic or Boolean algebra operations. The second overlaying approach uses one layer to identify boundaries by which information is extracted from other layers; that is, the value assigned to a thematic region is considered as a function of the values on other layers that occur within its boundary. Summary statistics may be applied to this approach.

### 1.2.3 Vector GIS and Capabilities

The traditional vector data model is based on vectors. Its fundamental primitive is a point. Lines are created by connecting points with straight lines, and areas are defined by sets of lines. Encoding these features (i.e., points, lines, and polygons) is based on Cartesian coordinates using the principles of Euclidean geometry. The more advanced topological vector model, based on graph theory, encodes

geographic features using nodes, arcs, and label points. The stretch of common boundary between two nodes forms an arc. Polygons are built by linking arcs or are stored as a sequence of coordinates. Figure 1.4 illustrates the arc-node topological data model.



**Point topology**

Pt ID	F. code
1	10001

Pt ID	Coord.
1	<i>xy</i>

**Arc topology**

Arc ID	F. code
21	20001
22	20300
23	20001
24	20400
...	

Arc ID	F node	T node
21	13	10
22	10	16
23	10	11
24	12	12
...		

Arc ID	Start	Intermediate	End
21	<i>xy</i>	<i>xy,xy,xy...</i>	<i>xy</i>
22	<i>xy</i>	<i>xy,xy,xy...</i>	<i>xy</i>
23	<i>xy</i>	<i>xy,xy,xy...</i>	<i>xy</i>
...			

**Polygon topology**

Poly ID	F. code
101	30200
102	40500
...	

Poly ID	Arcs list
101	30,32
102	24

Arc ID	F node	T node	L-poly	R-poly
24	12	12	103	102
30	14	15	World	101
32	14	15	101	105

Arc ID	Start	Intermediate	End
24	<i>xy</i>	<i>xy,xy,xy...</i>	<i>xy</i>
30	<i>xy</i>	<i>xy,xy,xy...</i>	<i>xy</i>
32	<i>xy</i>	<i>xy,xy,xy...</i>	<i>xy</i>

**FIGURE 1.4** The arc-node topological data model. (Adapted from Lo and Yeung, 2002; used with permission from Prentice Hall.)

The creation of a vector GIS database mainly involves three stages: (1) input of spatial data, (2) input of attribute data, and (3) linking of the spatial and attribute data.

The spatial data are entered via digitized points and lines, scanned, and via vectorized lines or directly from other digital sources. In the process of spatial data generation, once points are entered and geometric lines are created, topology must be built, which is followed by editing, edge matching, and other graphic spatial correction procedures. Topology is the mathematical relationship among the points, lines, and polygons in a vector data layer. Building topology involves calculating and encoding relationships between the points, lines, and polygons.

Attribute data

are data that describe the spatial features, which can be keyed in or imported from other digital databases. Attribute data often are stored and manipulated in entirely separate ways from the spatial data, with a linkage between the two types of data by a corresponding object ID. Various database models are used for spatial and attribute data in vector GIS. The most widely used one is the georelational database model (Fig. 1.5), which uses a common-feature identifier to link the topological data model, representing spatial data and their relationships, to a relational database management system (DBMS), representing attribute data.

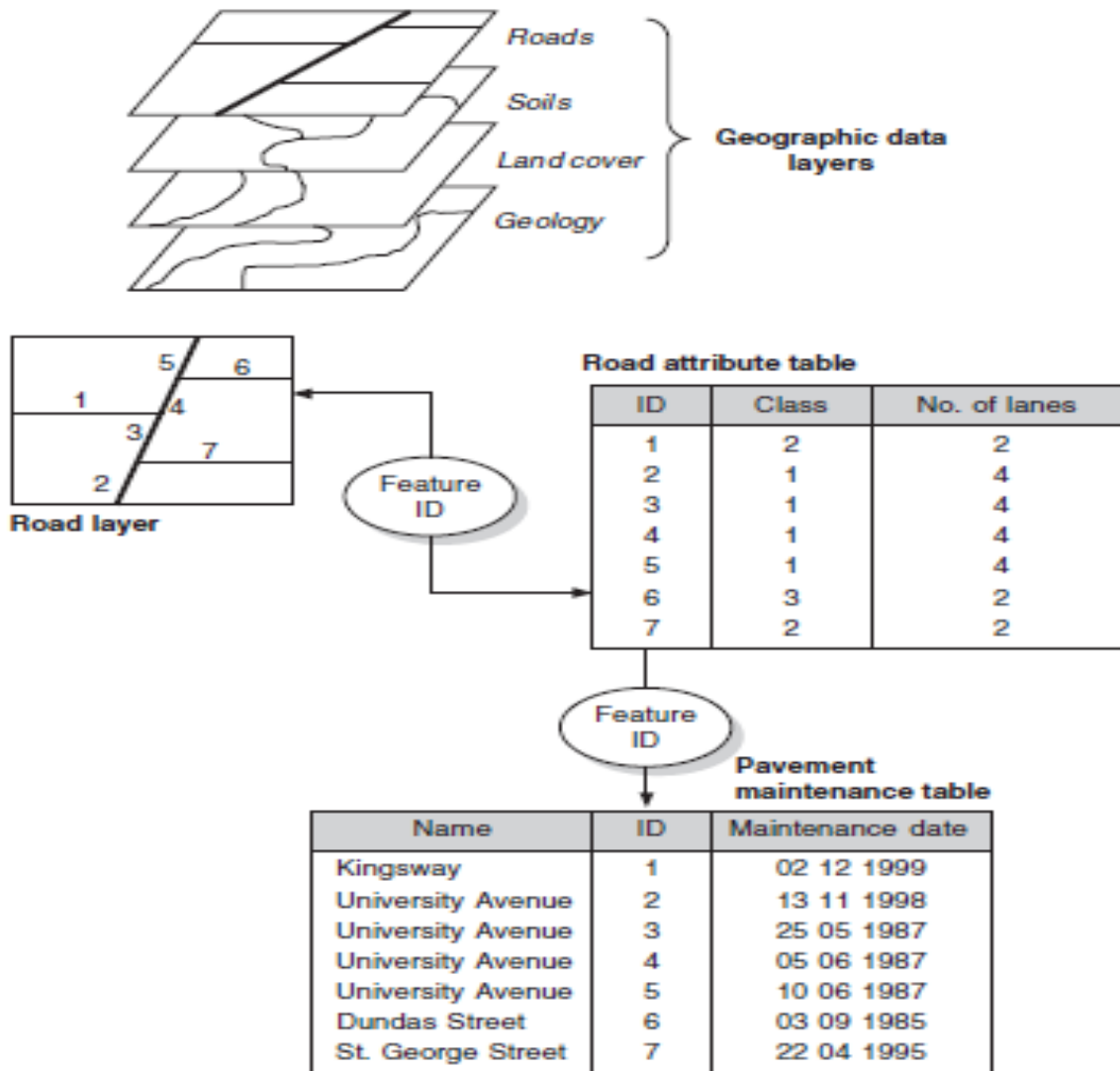
The analytical capabilities of vector GIS are not quite the same as those of raster GIS. There are more operations dealing with objects, and measures such as area have to be calculated from coordinates of objects instead of counting cells. The analytical functions can be broadly grouped into topological and nontopological ones.

The former includes buffering, overlay, network analysis, and reclassification, whereas the latter includes attribute database query, address geocoding, area calculation, and statistical computation (Lo and Yeung, 2002). Database query may be conducted according to the characteristics of the spatial or attribute data. Spatial queries may use points and arcs to display the locations of all objects stored or a subset of the data and may search within the radius of a point, within a bounding rectangle, or within an irregular polygon. Attributes and entity types can be displayed by varying colors, line patterns, or point symbols. Different vector GIS systems use different ways of formulating queries, but the Standard Query

Language (SQL), including relational, arithmetic, and Boolean operators, is used by many systems.

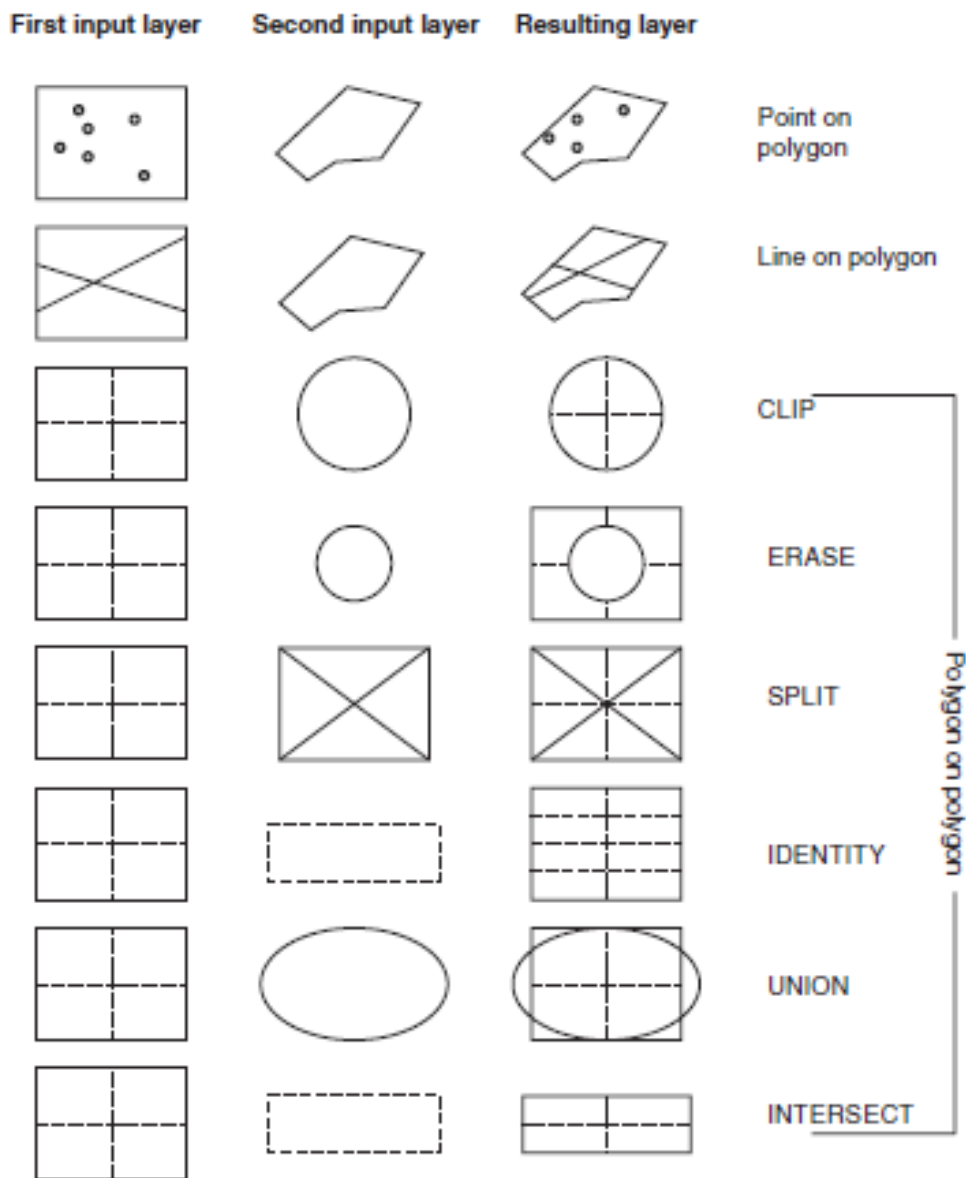
Topological overlay is an important vector GIS analytical function. When two GIS layers are overlaid, the topology is updated for the new, combined map. The result may be information about new relationships for the old (input) maps rather than the creation of new objects. Figure 1.6 shows various types of topological overlays.

The point-in-polygon overlay superimposes point objects on areas, thus computing “is contained in” relationship and resulting in a new attribute for each point. The line-on-polygon overlay superimposes line objects on area objects, thus computing “is contained in” relationships, and “containing area” is a new attribute of each output line.



**FIGURE 1.5** Georelational data model. The georelational data model stores graphical and attribute data separately. It makes use of common feature identifiers to link the data in different tables in the database. (Adapted from Lo and Yeung, 2002; used with permission from Prentice Hall.)

The polygon-on-polygon (i.e., polygon) overlay superimposes two layers of area objects. After overlaying, either of the input layers can be recreated by dissolving and merging based on the attributes contributed by the input layer. A buffer can be constructed around a point, line, or area, and buffering thus creates a new area enclosing the buffered object. Sometimes width of the buffer can be determined by an attribute of the object. Buffering may be applied to both vector and raster GIS and has found wide applications in transportation, forestry, resource management, etc.



**FIGURE 1.6** Types of topological overlay operations. (Adapted from Lo and Yeung, 2002; used with permission from Prentice Hall.)

# المحاضرة الحادية عشر

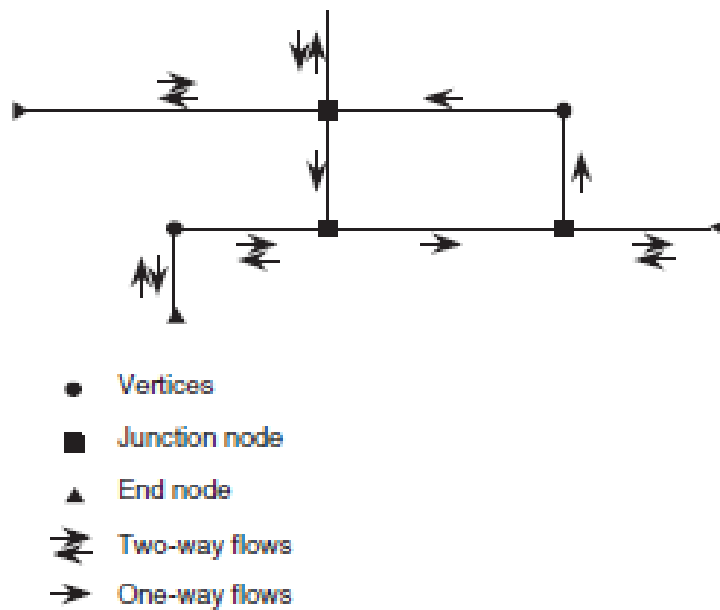
**Principle of Geographic Information System**



## Network Data Model

A network consists of a set of interconnected linear features. Examples of networks are roads, railways, air routes, rivers and streams, and utilities networks. In GIS, networks are modeled essentially by the arc-node topological data model, with attributes of links, nodes, stops, centers, and turns. To apply a network data model to real world applications, additional attributes such as travel time, impedance (e.g., cost associated with passing a link, stop, center, turn, etc), the nature of flow (i.e., one-way flow, two-way flow, close, etc.), and supply and demand must be included. Figure 1.7 provides an example of a network data model. Correct topology is of foremost importance for network analysis, but correct geographic representation is

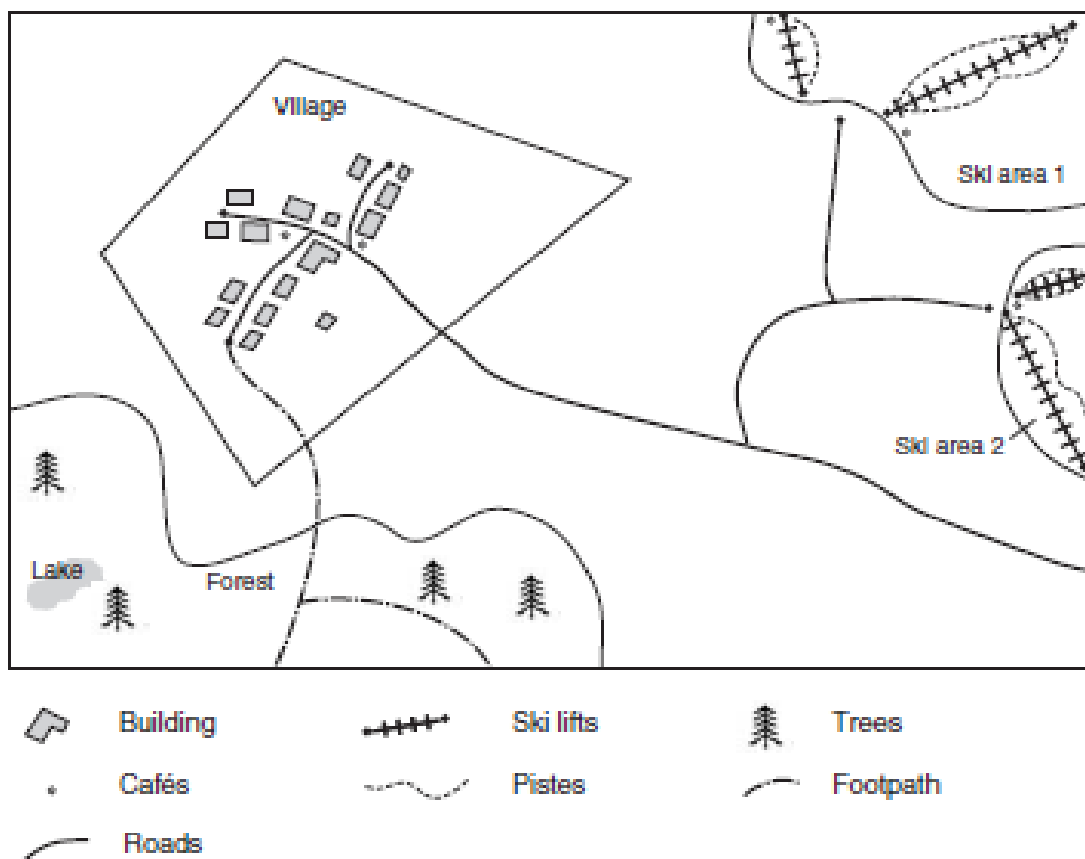
not so long as key attributes are preserved (Heywood et al., 1998). Applications that use a network data model include shortest-path analysis, location-allocation analysis, transportation planning, spatial optimization, and so on



**FIGURE 1.7** Network data model. (Adapted from Heywood et al. 1998; used with permission from Prentice Hall.)

## Object-Oriented Data Model

The concept of object orientation embraces four components: (1) object oriented user interface (e.g., icons, dialog boxes, glyphs, etc.), (2) object oriented programming languages (e.g., Visual Basic and Visual C), (3) object-oriented analysis, and (4) object-oriented database management (Lo and Yeung, 2002). The object-oriented data model discussed in most GIS textbooks focuses on the last two components. Unlike the georelational data model, which separates spatial and attribute data and links them by using a common identifier, the object-oriented data model views the real world as a set of individual objects. An object has a set of properties and can perform operations on requests (Chang, 2009). Figure 1.8 illustrates the object-oriented representation approach. Features are no longer divided into separate layers; instead, they are grouped into classes and hierarchies of objects.



**FIGURE 1.8** The object-oriented approach. (Adapted from Heywood et al. 1998; used with permission from Prentice Hall.)

The properties of each object include geographic information (e.g., size, shape, and location), topological information (i.e., one object relating to others), behaviors of the object, and behaviors of the objects in relation to one another. To apply the object-oriented data model to GIS, one must consider both the structural aspects of objects (Worboys, 1995) and behavior aspects of the objects (Egenhofer and Frank, 1992). Basic principles for explaining the structures of objects include association, aggregation, generalization, instantiation, and specialization, whereas those for explaining the behaviors of objects include inheritance, encapsulation, and polymorphism (Chang, 2009; Lo and Yeung, 2002).

# المحاضرة الثانية عشر

**DIGITAL IMAGE ANALYSIS**

## CHAPTER SIX

### DIGITAL IMAGE ANALYSIS

#### ***1. Introduction***

Digital image analysis refers to the manipulation of digital images with the aid of a computer.

This could range from an amateur photographer using freely available software to adjust the contrast and brightness of pictures from her or his digital camera to a team of scientists using neural-network classification to map mineral types in an airborne hyperspectral image.

In this lecture, we will begin with simple and widely used methods for enhancing digital images, correcting errors, and generally improving image quality prior to further visual interpretation or digital analysis.

The enhancement, processing, and analysis of digital images comprise an extremely broad subject, often involving procedures that can be mathematically complex.

The use of computers for digital processing and analysis began in the 1960s with early studies of airborne multispectral scanner data and digitized aerial photographs. However, it was not until the launch of Landsat-1 in 1972 that digital image data became widely available for land remote sensing applications. At that time, not only was the theory and practice of digital image processing in its infancy, but also the cost of digital computers was very high, and their computational efficiency was very low by modern standards.

Today, access to low-cost, efficient computer hardware and software is commonplace, and the sources of digital image data are many and varied.

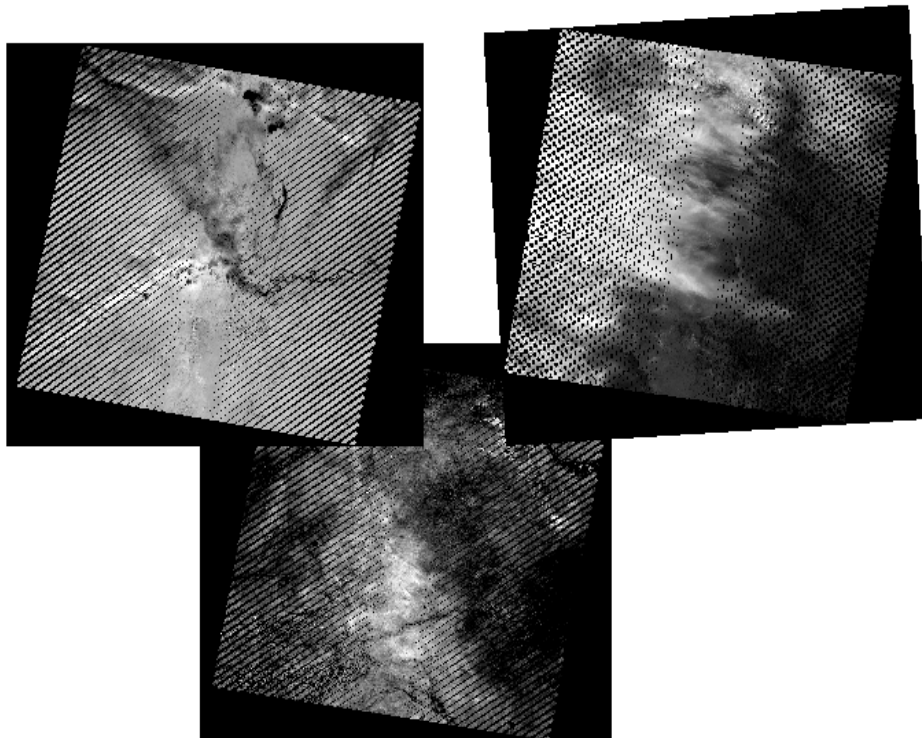
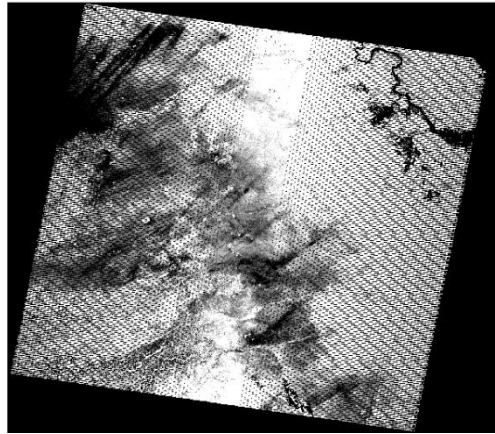
These sources range from commercial and governmental earth resource satellite systems, to the meteorological satellites, to airborne scanner data, to airborne digital camera data, to image data generated by photogrammetric scanners and other high resolution digitizing systems. All of these forms of data can be processed and analyzed using the techniques described in this chapter.

The central idea behind digital image processing is quite simple. One or more images are loaded into a computer. The computer is programmed to perform calculations using an equation, or series of equations, that take pixel values from the raw image as input. In most cases, the output will be a new digital image whose pixel values are the result of those calculations.

This output image may be displayed or recorded in pictorial format or may itself be further manipulated by additional software. However, virtually all these procedures may be categorized into one (or more) of the following seven broad types of computer-assisted operations:

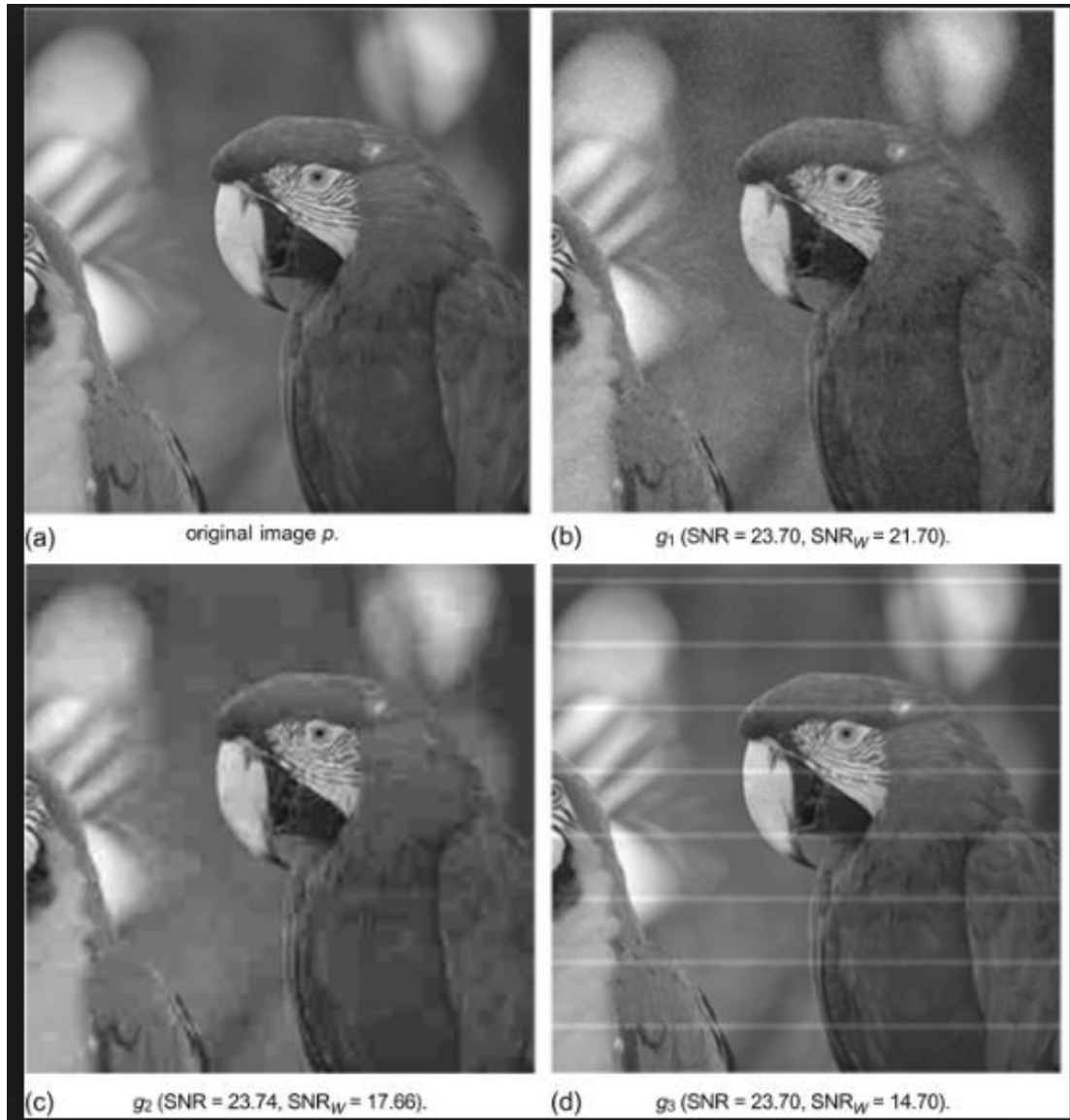
1. ***Image preprocessing.*** These operations aim to correct distorted or degraded image data to create a more faithful representation of the original scene and to improve an image's utility for further manipulation later on. This typically involves the initial processing of raw image data
  - to eliminate noise present in the data,
  - to calibrate the data radiometrically,
  - to correct for geometric distortions, and
  - to expand or contract the extent of an image via mosaicking or subsetting.

These procedures are often termed preprocessing operations because they normally precede further manipulation and analysis of the image data to extract specific information.



2. ***Image enhancement.*** These procedures are applied to image data in order to more effectively render the data for subsequent interpretation. In many cases, image enhancement involves techniques for

heightening the visual distinctions among features in a scene, ultimately increasing the amount of information that can be interpreted from the data.



There is various approaches to enhancement the images :

- the contrast of an image (level slicing and contrast stretching).



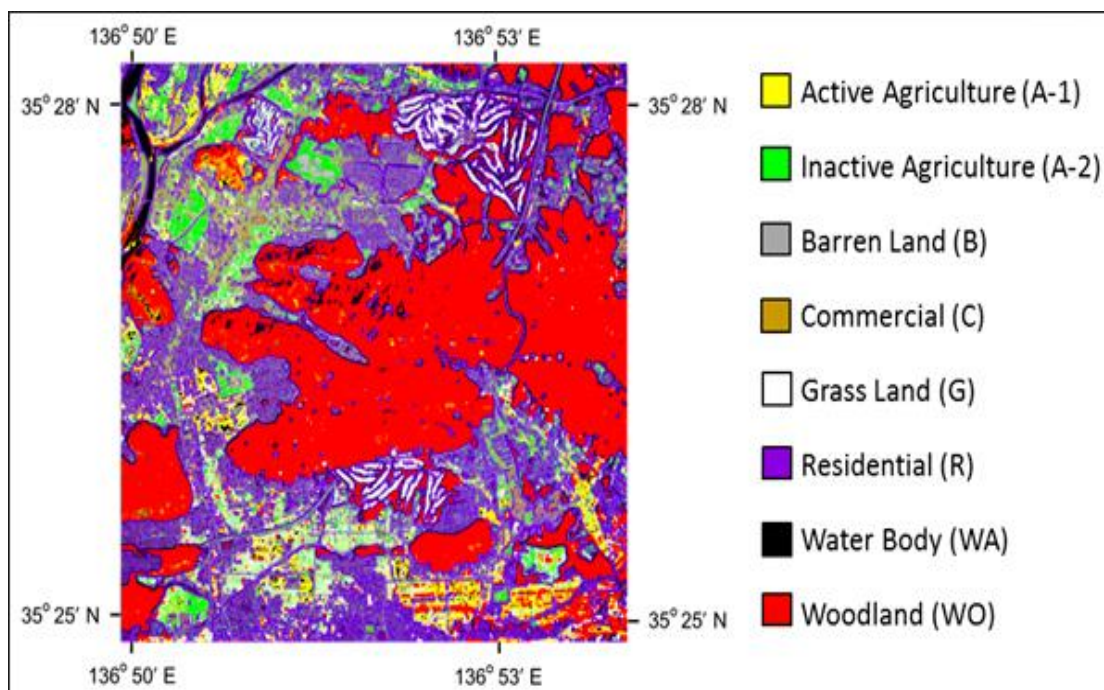
- spatial feature manipulation (spatial filtering, convolution, edge enhancement, and Fourier analysis).
- enhancements involving multiple spectral bands of imagery (spectral ratioing, principal and canonical components, vegetation components, and intensity–hue–saturation color space transformations).

# المحاضرة الثالثة عشر

DIGITAL IMAGE ANALYSIS

3. ***Image classification.*** The objective of image classification is to replace visual interpretation of image data with quantitative techniques for automating the identification of features in a scene.

This normally involves the analysis of multiple bands of image data (typically multispectral, multitemporal, or other sources of complementary information) and the application of statistically based decision rules for determining the land cover identity of each pixel in an image.



4. ***Analysis of change over time.*** Analysis of change over time. Many remote sensing projects involve the analysis of two or more images from different points in time, to determine the extent and nature of changes over time. Change detection methods are applied to identify specific areas of change. With the proliferation of temporally rich data sets that offer dozens or hundreds of images of a given area over a period of weeks or years, there is also a new interest in time-series analysis of remotely sensed imagery ,

such as the analysis of seasonal cycles, interannual variability, and long-term trends in dense multitemporal data sets.

**5. *Data fusion and GIS integration.*** These procedures are used to combine image data for a given geographic area with other geographically referenced data sets for the same area. These other data sets might simply consist of image data generated on other dates by the same sensor or by other remote sensing systems. Frequently, the intent of data merging is to combine remotely sensed data with other ancillary sources of information in the context of a GIS. For example, image data are often combined with soil, topographic, ownership, zoning, and assessment information.

**6. *Hyperspectral image analysis.*** Virtually all of the image processing principles introduced in this chapter in the context of multispectral image analysis may be extended directly to the analysis of hyperspectral data. However, the basic nature and sheer volume of hyperspectral data sets is such that various image processing procedures have been developed to analyze such data specifically.

**7. *Biophysical modeling.*** The objective of biophysical modeling is to relate quantitatively the digital data recorded by a remote sensing system to biophysical features and phenomena measured on the ground. For example, remotely sensed data might be used to estimate such varied parameters as crop yield, pollution concentration, or water depth. A biophysical model is a simulation of a biological system using mathematical formalizations of the physical properties of that system. Such models can be used to predict the influence of biological and physical factors on complex systems.

Remote sensing may be used to collect information on several important biophysical variables. This capability is in addition to the standard use of

remotely sensed data for land-use and land-cover mapping. The status of work on remotely sensing nine fundamental biophysical variables is presented, including planimetric (x, y) location, topographic-bathymetric (x, y, z) elevation, color and the spectral signature of features, vegetation chlorophyll absorption characteristics, vegetation biomass, vegetation moisture content, soil moisture content, surface temperature, and texture or surface roughness. Remotely sensed ratio-scaled data on these biophysical variables may be more amenable for use in models and simulations than the nominal-scale land-use data. Emphasis is placed on current remote sensing capability and future potential and on the optimum spectral region(s) for sensing these biophysical variables.

## ***2. Preprocessing of Images***

In nearly every case, there are certain preprocessing operations that are performed on the raw data of an image prior to its use in any further enhancement, interpretation, or analysis. Some of these operations are designed to correct flaws in the data, while others make the data more amenable to further processing. In this section we will discuss these preprocessing operations under the general headings of noise removal, radiometric correction, geometric correction, and image subsetting and mosaicking.

Some of these operations may be performed by the data provider, before the imagery is provided to the analysts who will be interpreting it. In other cases, the users may need to perform one or more of these preprocessing steps themselves.

# المحاضرة الرابعة عشر

Application of remote sensing in water resources

Presentation (project)